MINERALOGICAL CHARACTERIZATION OF STRATA OF THE MEADE PEAK PHOSPHATIC SHALE MEMBER OF THE PERMIAN PHOSPHORIA FORMATION

Channel and Individual Rock Samples of Measured Section J and Their Relationship to Measured Sections A and B, Central Part of Rasmussen Ridge, Caribou County, Idaho

by

A. C. Knudsen[1], M. E. Gunter[1], J. R. Herring[2], and R. I. Grauch[2]

Open-File Report 02-125

2001

Prepared in collaboration with
U.S. Bureau of Land Management
U.S. Forest Service
Agrium U.S. Inc.
Astaris LLC
J.R. Simplot Company
Rhodia Inc.
Monsanto

U. S. DEPARTMENT OF THE INTERIOR
U. S. GEOLOGICAL SURVEY

---

[1] Department of Geological Sciences, University of Idaho, Moscow, ID 83844-3022
[2] U.S. Geological Survey, Denver Federal Center, Box 25046, MS 973, Denver, CO 80225

CONTENTS

FIGURES

3 b: Quartz content of samples from the central part of Rasmussen Ridge, including the measured stratigraphic sections J (including channel and individual samples), B, and A.

3 c: Muscovite + illite content of samples from the central part of Rasmussen Ridge, including the measured stratigraphic sections J (including channel and individual samples), B, and A.

3 d: Total feldspar (albite + orthoclase + buddingtonite) content of samples from the central part of Rasmussen Ridge, including the measured stratigraphic sections J (including channel and individual samples), B, and A.

3 e: Buddingtonite content of samples from the central part of Rasmussen Ridge, including the measured stratigraphic sections J (including channel and individual samples), B, and A.

3 f: Dolomite content of samples from the central part of Rasmussen Ridge, including the measured stratigraphic sections J (including channel and individual samples), B, and A.

3 g: Calcite content of samples from the central part of Rasmussen Ridge, including the measured stratigraphic sections J (including channel and individual samples), B, and A.

4: Carbonate substitution for phosphate in fluorapatite reported in weight percent for samples from the central part of Rasmussen Ridge including the measured stratigraphic sections J (including channel and individual samples), B, and A. Carbonate content is determined using the equation of Schuffert and others (1990)

TABLES

1a: Quantitative mineralogy for section J channel samples calculated using the Rietveld method.

1b: Quantitative mineralogy for section J individual samples calculated using the Rietveld method.

2a: Data for CO_3^{2-} substitution in fluorapatite for section J channel samples based on the equation by Schuffert and others (1990).

2b: Data for CO_3^{2-} substitution in fluorapatite for section J individual samples based on the equation by Schuffert and others (1990).

ABSTRACT

The Permian Phosphoria Formation of southeastern Idaho hosts one of the largest phosphate deposits in the world. Despite the economic significance of this Formation, the fine-grained nature of the phosphorite has discouraged detailed mineralogical characterization and quantification studies. Recently, selenium and other potentially toxic trace elements in mine wastes have drawn increased attention to this formation, and motivated additional study. This study uses powder X-ray diffraction (XRD), with Rietveld quantification software, to quantify and characterize the mineralogy of composite channel samples and individual samples collected from the stratigraphic sections measured by the U.S. Geological Survey in the Meade Peak Member of the Permian Phosphoria Formation at the Enoch Valley mine on Rasmussen Ridge, approximately 15 miles northeast of Soda Springs, Idaho. These samples are from the deep, least-weathered drill core, section J, and channel samples from the less-weathered section B and more-weathered section A. Sections A and B were collected from benches exposed by mining.

The dominant minerals present in these samples are carbonate-fluorapatite, which is the ore mineral, quartz, muscovite, albite, orthoclase, the ammonium feldspar buddingtonite ($NH_4AlSi_3O_8$), dolomite, and calcite. Because of their potential for hosting trace elements such as Se, the presence of minor pyrite and sphalerite is also noteworthy. The variable degree of exposure that sections have undergone and their close proximity to each other allows for consideration of the effects of weathering on the mineralogy of the rocks. While much of the mineralogy is similar between all three sections, the carbonate minerals decrease with increased weathering. Analysis of the carbonate content in the carbonate-fluorapatite by Rietveld refinement shows relatively low carbonate content (2 – 3% (wt.) CO_3^{2-}) in the apatite structure relative to global phosphorites. Further analysis and interpretation of these data, and similar data from other mine sites, will be released in a later publication.

INTRODUCTION

Background

U.S. Geological Survey (USGS) geologists have studied the Permian Phosphoria Formation in southeastern Idaho and the Western U.S. Phosphate Field throughout much of the twentieth century. In response to a request by the U.S. Bureau of Land Management (BLM), a new series of resource and geoenvironmental studies was initiated by the USGS in 1998. Present studies involve many scientific disciplines within the USGS and consist of: (1) integrated, multidisciplinary research directed toward resource and reserve estimations of phosphate in selected 7.5-minute quadrangles; (2) host phases for elements and mineralogical and petrochemical characteristics; (3) mobilization and reaction pathways, transport, and disposition of potentially toxic trace elements associated with the occurrence, development, and use of phosphate rock; (4) geophysical signatures; and (5) improving the understanding of depositional origin.

To carry out these studies, the USGS formed cooperative research relationships with: two Federal agencies, BLM and the U.S. Forest Service (USFS), which are responsible for land management and resource conservation on public lands; and with five private companies currently leasing or developing phosphate resources in southeastern Idaho. The companies are Agrium U.S. Inc. (Rasmussen Ridge mine), Astaris LLC (Dry Valley mine), Rhodia Inc. (Wooley Valley mine-inactive), J.R. Simplot Company (Smoky Canyon mine), and Monsanto (Enoch Valley mine). Because raw data acquired during the project will require time to interpret, the data are released in open-file reports for prompt availability to other workers. The open-file reports associated with this series of resource and geoenvironmental studies are submitted to each of the Federal and industry collaborators for technical comment; however, the USGS is solely responsible for the data contained in the reports.

Location and General Geology

Samples for this study were collected from the Meade Peak phosphatic shale member of the Phosphoria Formation, a major source of phosphate in the Western Phosphate Field (figure 1). The study area is the Enoch Valley mine on Rasmussen Ridge in southeastern Idaho (figure 2), approximately 15 miles northeast of Soda Springs, in a region that has experienced phosphate mining over the past several decades and currently has four active phosphate mines. Related mineralogical studies were conducted at the Dry Valley mine (figure 2), where measured sections C and D were collected (Tysdal and others, 2000a: Herring and others, 2000a: Knudsen and others, 2001). Samples from the Enoch Valley mine were collected from 160- to 180-ft-thick sections, including the measured stratigraphic sections A (most-weathered) and B (weathered) along with the drill core, section J (least-weathered). A more detailed discussion of the Phosphoria Formation is given by McKelvey and others (1959). Service (1966) provided an

evaluation of the western phosphate industry in Idaho and a brief description of the mining history, ore occurrence, and geology. Cressman and Swanson (1964) discussed detailed stratigraphy and petrology of these same rock units in nearby southwestern Montana. Gulbrandsen and Krier (1980) discussed general aspects of the large and rich phosphorus resources in the Phosphoria Formation near Soda Springs. Gulbrandsen (1966, 1975, and 1979) also summarized bulk chemical compositional data for various stratigraphic units in the Phosphoria Formation.

Past research identified the major minerals in the Formation, including carbonate-fluorapatite, quartz, and dolomite, and a variety of sheet silicates and feldspars. Minor phases such as pyrite and sphalerite have also been identified in the deposit. These particular minerals are of interest because they contain Se, an element of geoenvironmental significance and concern. Samples from this report differ from those in previous studies in that they are taken from a deep core, section J, which is far less weathered. Also included in this report are both channel samples and individual samples taken from section J. Unlike the channel samples, the individual samples can be used to pinpoint mineralogical and geochemical variations over smaller intervals. The samples from section J are less weathered than any previously collected and are thus referred to in this report as least-weathered.

Correlation with Measured Sections

The Phosphoria Formation near the measured sections consists of three members, which in ascending order are the Meade Peak phosphatic shale member, the Rex Chert member, and the informally named cherty shale member (McKelvey and others, 1959; Montgomery and Cheney, 1967; Brittenham, 1976; Oberlindacher, 1990). The measured sections of this report focus on the Meade Peak phosphatic shale member. The Meade Peak unconformably overlies the Grandeur Tongue of the Permian Park City Formation, and the Triassic Dinwoody Formation overlies the cherty shale member of the Phosphoria.

This report provides mineralogical information for the rock sequences that were sampled from a core that was drilled at the Enoch Valley mine. The authors refer to the core as the measured section (or simply section) J; the samples are also referred to as wpsJ [western phosphate section J]. Two stratigraphic sections, A and B, of the Meade Peak at the Enoch Valley mine were also measured and described by the USGS (Tysdal and others, 1999). Descriptions of these measured sections are reported by Grauch and others (2001). The report by Herring and others (2001) provides and discusses the bulk chemistry of the same set of rock samples as this report. The three reports are best used together in a complementary fashion to obtain the descriptive, chemical, and mineralogical information about the rock sections.

Rather than use the more general unit names (A, B, C, D) applied to these strata in southeastern Idaho by Hale (1967, p. 152), informal terms such as “lower ore,” “middle waste,” “upper ore, and “upper waste” are used in descriptions of measured section J and sections A and B. Some informal bed names (for example, Cap Rock) used at the Enoch Valley mine are also used. For measured sections A and B, contacts in the lower ore and

waste units within the Meade Peak were selected by mine personnel, whereas contacts within the middle and upper waste zones generally were picked by USGS personnel to correspond to intervals of consistent lithology as described in the field. English units of measurement are used throughout this report to facilitate direct correspondence with units in the extensive historical literature on the Phosphoria and with current industry usage.

In previous work at each operating mine, USGS geologists measured, described, and sampled a pair of sections that are close but at different depths below the pre-mining land surface (Tysdal and others, 1999, 2000a, 2000b, 2000c; chemical data reported by Herring and others 1999, 2000a, 2000b, and 2000c, 2001; and mineralogy by Knudsen and others 2000 and 2001). This enables evaluation of important effects of alteration and weathering on rock geochemistry and mineralogy. One section from each pair is labeled more-weathered and the other less-weathered. The Meade Peak interval in section J, in which beds dip 45 to 60 degrees, extends from about 200 to 500 feet below the drill hole collar, and spans a greater depth range below the pre-mining surface than sections measured in open pit mines. The drill hole collar elevation is at 6987 ft. Sections A and B were measured along surfaces exposed by mining equipment and were much closer to the pre-mining ground surface. Section A was about 40 feet and section B about 120 feet below the pre-mining surface. Section A's location is N42° 53.04', W111° 24.66', section B is at N42° 52.97', W111° 24.68', and the collar of the vertical drill hole from which the core for section J was collected is at N42° 52.99', W111° 24.75'. Measurements of unit and bed thickness in the measured sections and in the core are true thickness of the strata at the sample sites; apparent thickness of dipping strata was corrected to true thickness. The sections were measured to provide stratigraphic context of selected rock units that were sampled for chemical and mineralogical analysis; however, no detailed descriptions were made of the strata in the sections. Stratigraphic units of the middle waste, for example, are shown as mainly mudstone, although interbeds of other rock types may be present.

Rocks of section J were cored prior to the start of mining, whereas rocks from all other measured sections were sampled at active mine exposures. Hence, the rocks from section J have not been affected by mining. Because phosphate mining commonly involves blasting, the absence of mining means that blasting has not fractured the rocks in section J.

Strata exposed in sections J, A, and B dip approximately 55 degrees westward, on the backlimb of a major anticline. The Meade Peak section in the drill core log is listed as having a dip of approximately 55 degrees, with a range from 45 to 60 degrees because of minor folding. In section B, mudstone between the two exposed phosphorite sequences contains a structurally thickened, poorly exposed zone that is interpreted to contain a low-angle thrust fault. The fault is approximately parallel to bedding and repeats nearly the entire lower ore zone, although the Fish-scale bed, the lowermost bed of the Meade Peak, is not repeated. Sections A and B and section J differ in thickness, chiefly because of likely structural thickening by faulting of the lower ore zone of section B.

METHODS

Sampling

The J core was shipped to the laboratories of the USGS in Denver, Colorado for description and sampling. The samples within the measured sections that were obtained for geochemical, petrological, and mineralogical analysis were scraped or chiseled in a consistent manner along a channel across each entire interval of apparently uniform lithology. Intervals range from 0.5 - 8.6 feet, and about 0.5 to 1 kg of rock was collected for each channel-sample interval. When possible, a sawed split of consistent shape was taken from the core throughout the entire interval. This provided a single representative sample of the entire interval. The choice of sampling intervals is intended to characterize strata of more or less uniform lithology and of a broad thickness that can be handled by typical mine equipment should the results of our analyses suggest that separate handling of such zones would be advantageous. Within these broad intervals, intervals as thin as a foot or less were sampled, where distinctly different lithologic units were noted. Individual samples may differ lithologically, geochemically, or mineralogically from the larger channel-sampled intervals from which they were taken. In some places, locations for the individual samples were guided by the results of hand-held XRF spectrometry analyses (Grauch and others, 2001). These analyses were obtained every 3 inches along the entire core - about 1100 measurements. The spectrometer produces a semi-quantitative analysis of a surface of about 2 cm^2 and has a detection limit ranging between about 20 and 150 ppm for As, Cr, Cu, Fe, Mn, Mo, Ni, Pb, Rb, Se, Sr, Zn, and Zr. Gamma rays emitted by this spectrometer penetrate less than a millimeter into the sample. Consequently, it is possible that the specific rock fragments analyzed are not representative of that interval.

Three suites of the individual samples were chosen to address the geochemical occurrence of organic carbon-rich zones within the dolostone of the Middle Waste Shale unit. Typically, these zones occur over about 3 to 4 feet of core. Each zone base begins with the appearance of tiny stringers of stratigraphically thin organic carbon seams or carbon-rich areas, a few millimeters to centimeters in thickness and with relatively sharp bedding contacts within the dolostone. The abundance and thickness of the stringers increases stratigraphically upward until there is a sharp termination of the stringers. XRF analyses of these zones indicate that concentrations of trace elements such as Se increase as the carbon seams become more abundant within the dolostone.

Rock Sample Preparation

Measured section J channel and individual samples were disaggregated in a mechanical jaw crusher, and then a representative split was ground in a ceramic plate grinder to <100 mesh (<0.15 mm). Representative splits of the latter material were provided to various collaborators, to the contract laboratory for chemical analysis, and to

the University of Idaho lab for mineralogical analysis. All splits were obtained with a riffle splitter to ensure similarity with the whole sample.

Analysis

XRD analyses were conducted with a 2-Theta scan from 2° - 62° over 28 minutes, using Cu radiation on a Siemens D5000 diffractometer operating at 40 kV and 30 mA. All samples were crushed to <100 mesh as described above. These relatively fast scans reveal the major phases in the samples; however, low peak to background ratios prevent accurate identification of minor phases, generally those less than 1%, depending a mineral phase's crystallinity and electron density. The patterns are subsequently analyzed using the Siroquant program (Taylor, 1991), which uses Rietveld analysis to quantify the mineralogical content in weight. First, every phase in a sample must be identified; the program then calculates an XRD pattern based on the known crystal structure of each mineral to match the actual pattern to determine the quantities of each phase. Siroquant refines the calculated pattern for each phase to match the collected pattern, correcting for variable peak shape, preferred orientation, and shifts in cell parameters. The quantity of each phase is reported along with an error value (tables 1a-b). The overall quality of the match between the calculated and collected patterns is shown by the statistical value "χ^2", where lower values represent better matches and any value under 3.0 is considered acceptable.

Measurement of the carbonate substitution in fluorapatite was done differently for this report than it had been done previously by Knudsen and others (2000 and 2001). In the two previous reports in this series, the carbonate content of the fluorapatite was estimated based on the measured fluorapatite a-cell parameter, based on the equation from McClellan (1980). However, for this method to be accurate an internal standard must be used, which was not done in the previous studies rendering them less accurate than the current study. McClellan (1980) based his formula on the observations of Smith and Lehr (1966) and McClellan and Lehr (1969) that as CO_3^{2-} enters the fluorapatite structure, the a-cell parameter shrinks, while the c-cell parameter stays relatively constant. Based on this same observation, Gulbrandsen (1970) derived a formula comparing the distance between the (004) and (410) diffraction peaks. In this method the location of each of these peaks is measured in degrees 2θ and then compared. Because this method compares the shifting a-cell parameter and the relatively constant c-cell parameter, any shifting in the diffraction pattern due to instrumental or preparation error is accounted for, and the need for an internal standard is eliminated. Later, Schuffert and others (1990) further refined this method to come up with the more accurate formula:

$$y = 10.643x^2 - 52.512x + 56.986.$$

Here y is the weight % of CO_3^{2-} present in the fluorapatite and x is the $\Delta 2\theta_{(004)\,-\,(410)}$. For this project, the method was improved slightly by calculating the (004) and (410) locations rather than measuring them. Using the Rietveld refinement, the a- and c-cell parameters were measured, and then used to calculate the location of the diffraction peaks. This method uses the measured cell parameters that are determined by an average of all diffraction peaks. It eliminates the possibility of mismeasurement of the peak

locations, which if mismeasured even by fractions of a degree can produce substantial errors.

RESULTS

Comparison of mineralogy between J channel samples and individual samples

The mineralogy of each measured section from the Enoch Valley mine is shown in figures 3a-g. Mineralogy of each major mineral species is shown in weight percent over the depth of the measured stratigraphic section in feet above the base of the Phosphoria Formation (he sample number). For channel samples, it is approximately the midpoint of the channel, while for individual samples it is the exact depth of the sample. As noted earlier the stratigraphy for these samples is given in Tysdal and others (2000b) for section J and Tysdal and others (1999) for sections A and B. The overall mineralogy of measured section J channel samples (table 1a) and individual samples (table 1b) offer few surprises in terms of bulk mineralogy in comparison to recent work (Knudsen and others, 2000 and 2001, Desborough and others 1999). The most prominent mineral species present are carbonate-fluorapatite, quartz, muscovite, albite, orthoclase, the ammonium feldspar buddingtonite ($NH_4AlSi_3O_8$), along with the carbonate minerals dolomite and calcite. Minor phases that host some trace elements such as Se include pyrite and sphalerite. Based on the sampling methodology described above, it is not surprising that the individual samples vary considerably from their host J channel samples (tables 1 a-b, figures 3 a-g). This variability emphasizes the mineralogical heterogeneity of the strata of the Meade Peak phosphatic shale. In each of the major mineral phases shown in figures 3 a-g, the mineralogical composition of the individual samples departs noticeably from the host channel samples. This serves as a reminder that the mineralogy for these and previously reported channel samples (Knudsen and others, 2000 and 2001) must be regarded as an average over a measured stratigraphic section.

Comparison of CO_3^{2-} substitution in fluorapatite between J channel samples and individual samples

The carbonate content in fluorapatite for section J samples is given in tables 2 a-b and then shown and compared to the carbonate content in sections A and B apatites in figure 4. Tables 2 a-b lists the weight percent CO_3^{2-} in the apatite structure, the percent apatite in the sample, as well as the lithology and the recognized ore or waste unit. Similar to figure 3, in figure 4 the percent of CO_3^{2-} in the apatite structure is shown over the depth of the measured stratigraphic sections measured in feet above the base of the Phosphoria Formation. Just as the bulk quantitative mineralogy varies between channel samples and individual samples, so too does the degree of carbonate substitution in apatite. While this variability is not surprising given the differences in bulk mineralogy between the sample sets, the difference is noteworthy. Controls on the concentration of carbonate in the fluorapatite structure are not well understood. Globally, CO_3^{2-} content in

carbonate-fluorapatite ranges from 2-3% in the Phosphoria Formation to 8-9% in phosphorite samples from Morocco (McArthur 1978). Further study of Meade Peak samples considering the variability of carbonate content between individual and channel samples as well as between sections, could yield a better understanding of the controls on the carbonate content, and the relative importance of depositional and weathering processes.

Mineralogical comparison of J channel samples with A- and B-Section samples

Analysis of the deep, least-weathered, section J provides an opportunity to examine the spatial variability of mineralogy locally and the possible effects of weathering and mining operations on the rocks. The most notable trend in the series of analyses of least-, less-, and more-weathered sections is the depletion of dolomite in the samples with increased weathering (figure 3f). In section J, identified here as the least-weathered, dolomite constitutes a major mineral throughout the section; however, in the less-weathered section B, dolomite is present primarily in the lower portion of the Middle Waste and throughout the Lower Ore Zone. Finally, in the more-weathered section A dolomite is rare. The disappearance of calcite with weathering is also notable (figure 3g). In the least-weathered section J, calcite makes up a considerable portion of some samples, particularly those from the Middle Waste where two samples contain more than 50% calcite. In the less-weathered section B, calcite is rare except for a few samples with minor calcite in the Middle Waste. Again, in the more-weathered section A, there is essentially no calcite. The significant variability in concentrations of dolomite and calcite between section J and the nearby sections A and B may be due partially to spatial variability or to structural elimination of carbonate-bearing strata between section J and sections A and B. However, this variability appears more likely to be a function of weathering. The easily weathered carbonate minerals decrease in concentration as weathering increases from the bottom of the least-weathered section J through the top of the more-weathered A section. This can be seen across the three sections, particularly within the less-weathered B section in which dolomite occurs in the deeper less-exposed Lower Ore but not in the shallower more-exposed Upper Ore.

The spatial distribution of buddingtonite between section J and the A and B sections is also interesting (figure 3e). While very little research has been done to understand the stability and dissolution kinetics of buddingtonite, the authors hypothesize that this unusual mineral may be susceptible to weathering because of the presumed instability of ammonium in the feldspar structure. Thus, we expected to observe higher quantities of buddingtonite in these relatively unaltered samples than had been previously reported in the more- and less- weathered sections (Knudsen and others, 2000 and 2001). However, it appears that the relative concentration of buddingtonite increases as weathering increases (figure 3e). While buddingtonite may be susceptible to weathering, it appears to be far less vulnerable than the carbonates and consequently increases in relative concentration closer to the surface.

The presence of carbonate within the apatite structure is not considered to be a robustly stable substitution, and upon exposure to weathering it has been observed that

the CO_3^{2-} is leached from the apatite structure (Lucas and others, 1979), though little variability in the content of CO_3^{2-} in fluorapatite between the three sections is seen (figure 4). The degree to which the progressively more weathered sections J, B, and A have been altered appears not to have been sufficient to significantly impact the relative content of CO_3^{2-} in apatite between the sections.

The results of this report are preliminary. Further consideration of these data, combined with mineralogical and geochemical data from studies of other sites in the region will result in more thorough interpretations on the effects of spatial and weathering variability on the nature of the Meade Peak phosphatic shale.

REFERENCES CITED

Brittenham, M.D., 1976, Permian Phosphoria carbonate banks, Idaho-Wyoming thrust belt, *in* Hill, J.G., ed., Symposium on geology of the Cordilleran hingeline: Rock Mountain Association of Geologists—1976 symposium, Denver, p. 173-191.

Cressman, E.R., and Swanson, R.W., 1964, Stratigraphy and petrology of the Permian rocks of southwestern Montana: U.S. Geological Survey Professional Paper 313-C, p. 275-569.

Desborough, G.A., DeWitt, E., Jones, J., Meier, A., and Meeker, G., 1999, Preliminary mineralogical and chemical studies related to the potential mobility of selenium and associated elements in Phosphoria formation strata, southeastern Idaho: U.S. Geological Survey Open-file Report 99-129, 20 p.

Grauch, R.I., Tysdal R.G, Johnson, E.A., Herring, J.R., and Desborough, G.A., 2001, Stratigraphic section and selected semiquantitative chemistry, Meade Peak Phosphatic Shale Member of Permian Phosphoria Formation, central part of Rasmussen Ridge, Caribou County, Idaho: U.S. Geological Survey Open-file Report 99-20-E.

Gulbrandsen, R.A., 1966, Chemical composition of phosphorites of the Phosphoria Formation: Geochimica et Cosmochimica Acta, v. 30, no. 8, p. 769-778.

---, 1970, Relation of carbon dioxide content of apatite of the Phosphoria Formation to the regional facies: U.S. Geological Survey Professional Paper 700-B p. 9-13.

---, 1975, Analytical data on the Phosphoria Formation, western United States: U.S. Geological Survey Open-File Report 75-554, 45 p.

---, 1979, Preliminary analytical data on the Meade Peak member of the Phosphoria Formation at Hot Springs underground mine, Trail Canyon trench, and Conda underground mine, southeastern Idaho: U.S. Geological Survey Open-File Report 79-369, 35 p.

Gulbrandsen, R.A., and Krier, D.J., 1980, Large and rich phosphorus resources in the Phosphoria Formation in the Soda Springs area southeastern Idaho: U.S. Geological Survey Bulletin 1496, 25 p.

Hale, L.A., 1967, Phosphate exploration using gamma radiation logs, Dry Valley, Idaho, in Hale, L.A., ed., Anatomy of the western phosphate field: Salt Lake City,

Intermountain Association of Field Geologists, 15th Annual Field Conference Guidebook, p. 147-159.

Herring, J.R., 1995, Permian phosphorites; a paradox of phosphogenesis *in*, Scholle, P.A., Peryt, T.M. and Ulmer-Scholle, D.S., editors, The Permian of northern Pangea; Volume 2, Sedimentary basins and economic resources, p. 292-312.

Herring, J.R., Desborough, G.A., Wilson, S.A., Tysdal, R.G., Grauch, R.I., and Gunter, M.E., 1999, Chemical composition of weathered and unweathered strata of the Meade Peak Phosphatic Shale Member of the Permian Phosphoria Formation--A. Measured sections A and B, central part of Rasmussen Ridge, Caribou County, Idaho: U.S. Geological Survey Open-File Report 99-147-A, 24 p.

Herring, J.R., Wilson, S.A., Stillings, L.A., Knudsen, A.C., Gunter, M.E., Tysdal, R.G., Grauch, R.I., Desborough, G.A., and Zielinski, R.A., 2000a, Chemical composition of weathered and less weathered strata of the Meade Phosphatic Shale Member of the Permian Phosphoria Formation—B. Measured sections C and D, Dry Valley, Caribou County, Idaho: U.S. Geological Survey Open-File Report 99-147-B, 34 p.

Herring, J.R., Grauch, R.I., Desborough, G.A., Wilson, S.A., and Tysdal, R.G., 2000b, Chemical composition of weathered and less weathered strata of the Meade Peak Phosphatic Shale Member of the Permian Phosphoria Formation—C. Measured sections E and F, Rasmussen Ridge, Caribou County, Idaho: U.S. Geological Survey Open-File Report 99-147-C, 35 p.

Herring, J.R., Grauch, R.I., Tysdal, R.G., Wilson, S.A., and Desborough, G.A., 2000c, Chemical composition of weathered and less weathered strata of the Meade Peak Phosphatic Shale Member of the Permian Phosphoria Formation—D. Measured sections G and H, Sage Creek area of the Webster Range, Caribou County, Idaho: U.S. Geological Survey Open-File Report 99-147-D, 38 p.

Herring, J.R., Grauch, R.I., Seims, D.F., Tysdal, R.G., Johnson, E.A., Zielinski, R.A. Desborough, G.A., Knudsen, A.C., and Gunter, M.E., 2001, Chemical composition of strata of the Meade Peak phosphatic shale member of the Permian Phosphoria Formation channel-composited and individual rock samples of measured section J and their relationship to measured sections A and B, central part of Rasmussen Ridge, Caribou County, Idaho: U.S. Geological Survey Open-File Report 01-195, 72 p.

Knudsen, A.C., Gunter, M.E., and Herring, J.R., 2000, Preliminary mineralogical characterization of weathered and less-weathered strata of the Meade Peak Phosphatic Shale Member of the Permian Phosphoria Formation: Measured sections A and B, central part of Rasmussen Ridge, Caribou County, Idaho: U.S. Geological Survey Open-File Report 00-116, 74 p.

---, 2001, Preliminary mineralogical characterization of weathered and less-weathered strata of the Meade Peak Phosphatic Shale Member of the Permian Phosphoria Formation: Measured sections C and D, Dry Valley, Caribou County, Idaho: U.S. Geological Survey Open-File Report 01-072, 72 p.

Lucas, J., Prèvôt, L., and El. Mountassir, M., 1979, Les phosphorites rubéfiées de Sidi Daoui. Transformation météorique locale du gisement de phosphate des Ouled Abdoun (Maroc). Sci Geol Bull v. 32 p. 21-37.

McArthur, J.M., 1978, Systematic variations in the contents of Na, Sr, CO_3, and SO_4 in marine carbonate fluorapatite and their relation to weathering: Chemical Geology, v. 21, p. 89-112.

McClellan, G.H., 1980, Mineralogy of carbonate fluorapatites: Geological Society of London, v. 137, p. 675-681.

McClellan, G.H., and Lehr, J.R., 1969, Crystal chemical investigation of natural apatites: American Mineralogist, v. 54, p. 1379-1391.

McKelvey, V.E., Williams, J.S., Sheldon, R.P., Cressman, E.R., Cheney, T.M., and Swanson, R.W., 1959, The Phosphoria, Park City, and Shedhorn Formations in the Western Phosphate Field: U.S. Geological Survey Professional Paper 313-A, 47 p.

Montgomery, K.M., and Cheney, T.M., 1967, Geology of the Stewart Flat quadrangle, Caribou County, Idaho: U.S. Geological Bulletin 1217, 63 p.

Oberlindacher, H.P., 1990, Geologic map and phosphate resources of the northeastern part of the Lower Valley quadrangle, Caribou County, Idaho: U.S. Geological Survey Miscellaneous Field Studies Map MF-2133, scale 1:12,000.

Schuffert, J.D., Dastner, M., Emanuele, G., and Jahnke, R.A., 1990, Carbonate-ion substitution in francolite: A new equation: Geochimica Cosmochimica Acta, v. 54, p. 2323-2328.

Service, A.L., 1966, An evaluation of the western phosphate industry and its resources, Part 3, Idaho: U.S. Bureau of Mines Report of Investigations 6801, 201 p.

Smith, J.P., and Lehr, J.R., 1966, An x-ray investigation of carbonate apatite: Journal of Agricultural Food Chemistry, v. 14, p. 342 – 349.

Taylor, J.C., 1991, Computer programs for standardless quantitative analysis of minerals using the full powder diffraction profile: Powder Diffraction, vol. 6, p. 2-9.

Tysdal, R.G., Johnson, E.A., Herring, J.R., and Desborough, G.A., 1999, Stratigraphic sections and equivalent uranium (eU), Meade Peak Phosphatic Shale Member of the Permian Phosphoria Formation, central part of Rasmussen Ridge, Caribou County, Idaho: U.S. Geological Survey Open-File Report 99-20-A.

Tysdal, R.G., Herring, J.R., Desborough, G.A., Grauch, R.I., and Stillings, L.A., 2000a, Stratigraphic sections and equivalent uranium (eU), Meade Peak Phosphatic Shale Member of Permian Phosphoria Formation, Dry Valley, Caribou County, Idaho: U.S. Geological Survey Open-File Report 99-20-B.

Tysdal, R.G., Grauch, R.I., Desborough, G.A., and Herring, J.R., 2000b, Stratigraphic sections and equivalent uranium (eU), Meade Peak Phosphatic Shale Member of the Permian Phosphoria Formation, east-central part of Rasmussen Ridge, Caribou County, Idaho: U.S. Geological Survey Open-File Report 99-20-C.

Tysdal, R.G., Herring, J.R., Grauch, R.I., Desborough, G.A., and Johnson, E.A., 2000c, Stratigraphic sections and equivalent uranium (eU), Meade Peak Phosphatic Shale Member of Permian Phosphoria Formation, Sage Creek area of Webster Range, Caribou County, Idaho: U.S. Geological Survey Open-file Report 99-20-D.

Figure 1: Map of the Western United States showing the Western Phosphate Field

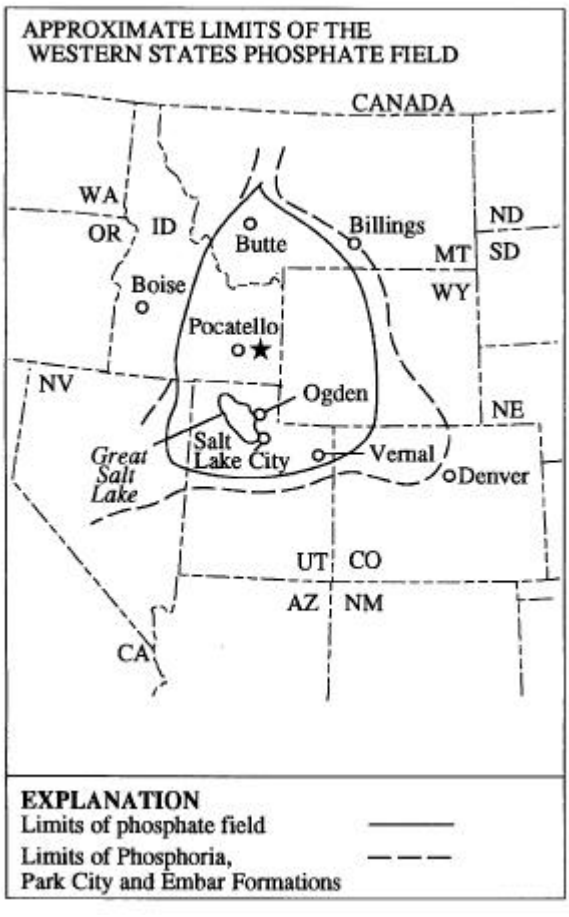

Figure 2: Index map of southeastern Idaho showing location of measured sections J, A, and B at the Enoch Valley mine from the central part of Rasmussen Ridge. The site of measured sections C and D is also shown at the Dry Valley mine.

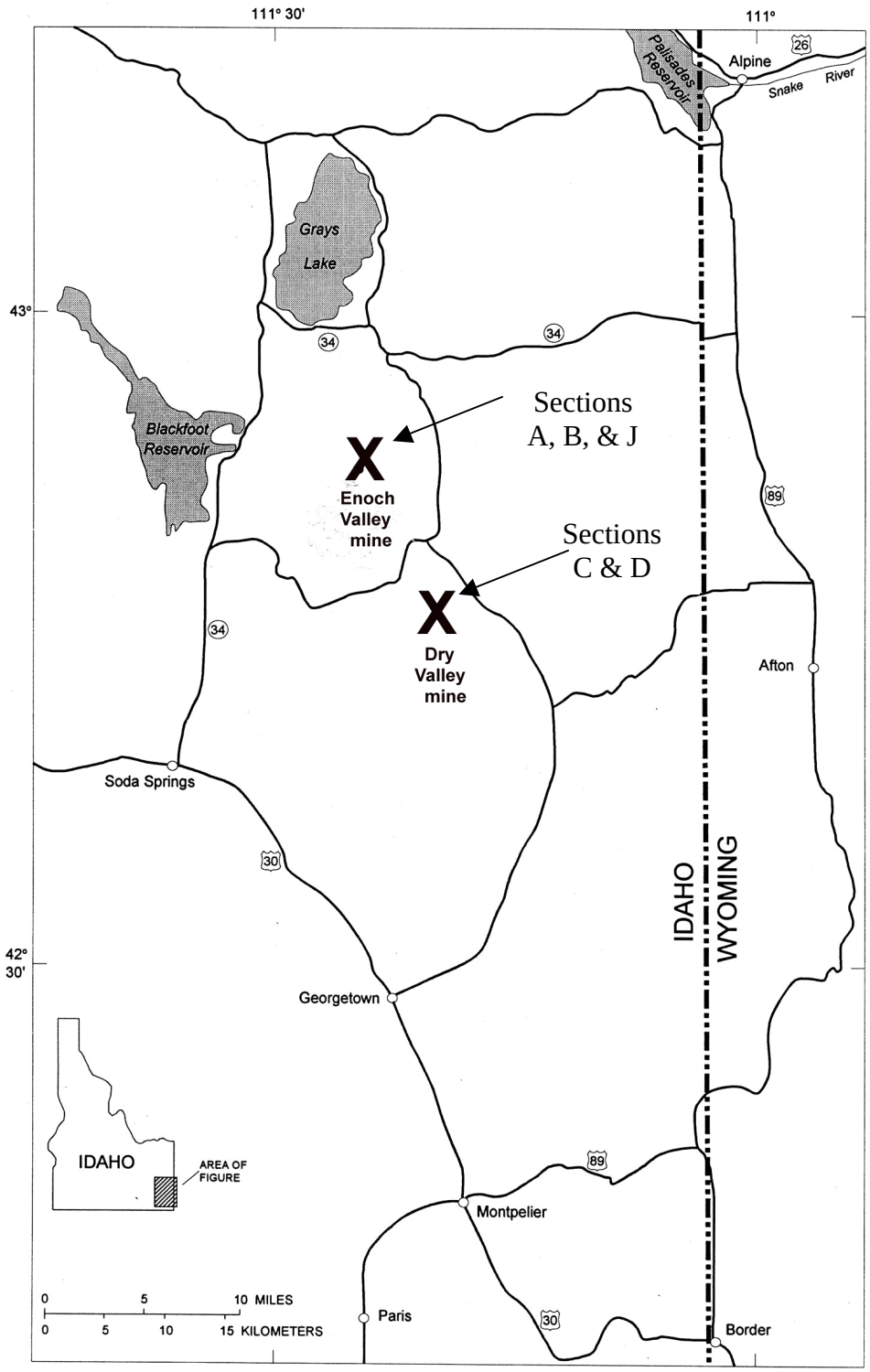

Table 1a: Quantitative mineralogy for section J channel samples calculated using the Rietveld method. The χ^2 value is a numerical statement of the quality of the match between the collected XRD pattern and the calculated Rietveld pattern where any value less than 3 is considered acceptable, with smaller χ^2 values inferring better results. Weight percents are listed with an accepted error in the last decimal place given in parentheses.

Sample	χ^2	Unit	Lithology	apatite	quartz	muscovite	illite	albite	orthoclase	buddingtonite	dolomite	calcite	pyrite
wpsJ187C	1.36	Rex Chert	chert	2 (3)	94 (1)	0.3 (5)	0.2 (4)	0.2 (3)	1.8 (4)	0.7 (4)	0.0 (2)	0.4 (2)	0.0 (1)
wpsJ186C	1.50	Upper Waste	phosphorite	61 (1)	31.8 (7)	3 (1)	0.1 (9)	0.1 (6)	0.1 (8)	2.5 (8)	0.0 (4)	0.0 (3)	0.5 (2)
wpsJ184C	1.82	Upper Waste	mudstone	7.6 (5)	57 (1)	15 (1)	5.2 (9)	2.3 (7)	1.9 (9)	3 (1)	1.2 (4)	1.0 (3)	3.5 (3)
wpsj181C	1.58	Upper Waste	mudstone	3.4 (6)	68 (2)	14 (1)	6 (1)	2.9 (8)	0 (1)	0 (1)	0.7 (5)	0.0 (4)	3.9 (3)
wpsJ177C	1.88	Upper Waste	mudstone	3.2 (5)	49 (1)	15 (1)	1.7 (8)	14.0 (6)	4.1 (7)	1.6 (7)	5.8 (4)	1.1 (3)	3.5 (2)
wpsJ175C	1.85	Upper Waste	mudstone	10.0 (6)	44 (1)	14 (1)	0.1 (9)	6.9 (6)	4.2 (7)	0.0 (7)	13.9 (5)	0.0 (3)	4.4 (2)
wpsJ172C	1.84	Upper Waste	mudstone	1.8 (4)	35.4 (8)	13 (1)	0.9 (7)	5.7 (6)	0.6 (5)	2.0 (5)	39.4 (9)	0.0 (3)	0.5 (2)
wpsJ170C	1.85	Upper Waste	mudstone	14.6 (7)	47 (1)	20 (2)	2 (1)	6.8 (7)	3.9 (8)	1.4 (8)	0.8 (4)	0.0 (3)	3.5 (2)
wpsJ169C	2.16	Upper Waste	siltstone	5.5 (5)	65 (2)	2 (2)	6 (1)	7.0 (7)	5.5 (9)	4.1 (8)	0.4 (4)	0.2 (3)	2.2 (2)
wpsJ168C	1.48	Upper Waste	phosphorite	44.2 (6)	51.0 (7)	0.8 (4)	0.2 (6)	0.3 (4)	0.4 (5)	1.1 (5)	0.1 (3)	0.2 (2)	0.9 (2)
wpsJ164C	1.99	Upper Waste	mudstone	6.5 (6)	55 (1)	19 (1)	0 (1)	13.4 (7)	0.1 (9)	1.3 (8)	0.8 (4)	0.0 (4)	3.8 (3)
wpsJ163C	1.42	Upper Ore	phosphorite	85 (2)	11.7 (3)	1.0 (8)	0.1 (9)	1.1 (6)	0.1 (7)	0.1 (8)	0.3 (4)	0.0 (3)	0.2 (2)
wpsJ162C	1.25	Upper Ore	phosphorite	92 (2)	4.7 (3)	1 (1)	0.5 (8)	0.1 (6)	0.1 (6)	0.2 (7)	0.0 (4)	0.3 (3)	1.0 (2)
wpsJ161C	1.43	Upper Ore	phosphorite	92 (2)	5.7 (3)	0.8 (1)	0.7 (9)	0.1 (6)	0.1 (7)	0.1 (8)	0.0 (4)	0.0 (3)	0.1 (2)
wpsJ160C	1.48	Upper Ore	phosphorite	81 (2)	5.1 (3)	12 (2)	0.1 (8)	0.9 (6)	0.1 (6)	0.1 (7)	0.0 (3)	0.0 (3)	0.0 (2)
		Upper Ore											
wpsJ159C	1.49	Upper Ore	phosphorite	55 (1)	25.6 (7)	8 (1)	1 (1)	5.6 (9)	0.8 (8)	3 (1)	0.0 (4)	0.3 (3)	1.6 (3)
wpsJ158C	1.44	Upper Ore	phosphorite	83 (2)	9.3 (3)	3.4 (2)	1.4 (8)	1.4 (6)	0.1 (7)	0.1 (7)	0.0 (4)	0.2 (3)	0.7 (2)
wpsJ156C	1.35	Upper Ore	phosphorite	90 (2)	9.2 (4)	0.0 (1)	0.1 (8)	0.6 (6)	0.1 (6)	0.1 (7)	0.0 (2)	0.0 (3)	0.0 (2)
wpsJ155C	1.38	Upper Ore	phosphorite	92 (1)	5.8 (2)	1.2 (1)	0.1 (8)	0.1 (6)	0.1 (6)	0.1 (7)	0.1 (2)	0.0 (3)	0.6 (2)
wpsJ154C	1.63	Upper Ore	phosphorite	80 (2)	9.1 (4)	8 (2)	0 (1)	0.1 (7)	0.1 (7)	0.1 (8)	0.1 (2)	0.0 (4)	1.9 (3)
wpsJ153C	1.45	Upper Ore	phosphorite	76 (2)	12.5 (4)	10 (2)	0.1 (9)	0.1 (6)	0.1 (7)	0.1 (7)	0.1 (2)	0.0 (3)	0.7 (2)
wpsJ151C	1.61	Upper Ore	phosphorite	62 (2)	16.3 (7)	10 (2)	8 (2)	0.1 (8)	0 (1)	0.1 (9)	0.0 (3)	0.0 (4)	2.2 (3)
wpsJ150C	1.44	Upper Ore	phosphorite	70 (2)	14.9 (5)	8 (2)	1.0 (8)	2.5 (6)	1.3 (7)	0.1 (7)	0.1 (2)	0.0 (3)	2.1 (2)
wpsJ149C	1.54	Upper Ore	phosphorite	62 (2)	16.1 (5)	6 (1)	0.1 (8)	3.2 (6)	0.1 (9)	10 (2)	0.0 (2)	0.0 (3)	2.1 (2)
wpsJ148C	1.54	Middle Waste	siltstone	39 (1)	32.3 (8)	15 (1)	0.1 (9)	1.5 (4)	0.1 (7)	8 (1)	0.4 (2)	0.0 (3)	2.8 (3)

Table 1a: (continued)

Sample	χ^2	Unit	Lithology	apatite	quartz	muscovite	illite	albite	orthoclase	buddingtonite	dolomite	calcite	pyrite
wpsJ147C	1.69	Middle Waste	mudstone	25.3 (8)	40 (1)	13 (1)	2 (1)	4.8 (7)	6.4 (8)	6.1 (9)	0.8 (2)	0.7 (4)	1.1 (3)
wpsJ145C	1.78	Middle Waste	siltstone	35 (1)	35 (1)	11 (1)	0 (1)	5.6 (8)	1.1 (9)	7 (1)	1.0 (2)	0.0 (4)	3.7 (3)
wpsJ143C	1.76	Middle Waste	siltstone	25.3 (6)	43.8 (8)	5.9 (2)	3 (8)	4.2 (6)	0.1 (8)	10.7 (7)	1.8 (2)	0.0 (3)	4.6 (2)
wpsJ140C	1.64	Middle Waste	mudstone	40 (1)	32.3 (8)	10 (1)	0.1 (9)	3.4 (6)	1.0 (8)	9.7 (9)	0.7 (2)	0.0 (3)	3.1 (2)
wpsJ136C	1.71	Middle Waste	mudstone	29.1 (8)	31.9 (8)	7 (1)	0.1 (8)	6.2 (6)	2 (1)	9.4 (9)	7.2 (5)	0.0 (3)	6.5 (3)
wpsJ131C	1.71	Middle Waste	siltstone	32.7 (7)	26.3 (5)	7.8 (9)	0.1 (7)	7.0 (5)	2.4 (6)	10.7 (8)	5.9 (4)	2.5 (2)	4.3 (2)
wpsJ128C	1.71	Middle Waste	siltstone	4.2 (4)	17.8 (4)	1 (1)	0.1 (6)	10.5 (6)	1.7 (5)	8.6 (7)	50 (1)	3.3 (2)	2.9 (2)
wpsJ125C	1.66	Middle Waste	mudstone	9.4 (5)	49.3 (8)	4.4 (3)	0.1 (7)	10.4 (5)	15.3 (6)	1.4 (4)	5.0 (3)	0.0 (2)	3.4 (2)
wpsJ123C	1.56	Middle Waste	mudstone	52 (1)	31.1 (6)	8 (1)	0.9 (7)	0.9 (4)	2.2 (5)	0.8 (3)	0.1 (3)	0.0 (2)	1.8 (2)
wpsJ121C	1.86	Middle Waste	mudstone	28.0 (6)	42.8 (7)	1.7 (8)	2.0 (7)	5.3 (4)	7.1 (5)	9.5 (6)	0.0 (3)	0.0 (2)	3.3 (2)
wpsJ117C	1.56	Middle Waste	mudstone	32.3 (7)	37.3 (7)	6.1 (9)	0.8 (7)	6.3 (6)	1.1 (6)	11.6 (8)	0.0 (2)	0.0 (2)	2.7 (2)
wpsJ114C	1.69	Middle Waste	mudstone	35.9 (8)	32.9 (7)	7 (1)	0.1 (8)	8.1 (6)	0.1 (3)	11.0 (9)	0.0 (4)	0.0 (3)	3.3 (2)
wpsJ111C	1.78	Middle Waste	phosphorite	14.8 (6)	34.7 (7)	13.6 (7)	0.3 (8)	4.5 (5)	0.1 (6)	19 (1)	6.1 (3)	2.9 (2)	2.9 (2)
wpsJ106C	1.73	Middle Waste	mudstone	19.3 (7)	33.6 (8)	9 (1)	0.3 (8)	8.3 (5)	2.3 (7)	10.1 (8)	3.3 (9)	8.4 (8)	4.2 (3)
wpsJ102C	1.67	Middle Waste	mudstone	25.6 (8)	14.7 (5)	12 (1)	0.8 (8)	2.5 (6)	0.1 (8)	21 (1)	5.2 (3)	12.1 (4)	6.6 (3)
wpsJ098C	1.42	Middle Waste	dolostone	1.0 (5)	2.2 (3)	0.1 (4)	0.1 (6)	1.2 (4)	1.4 (6)	8.8 (9)	62 (1)	22.2 (6)	1.3 (2)
wpsJ095C	1.52	Middle Waste	mudstone	18.7 (5)	10.4 (3)	7.8 (5)	0.1 (8)	2.4 (5)	0.1 (7)	13.0 (8)	16.9 (3)	26.3 (5)	3.2 (2)
wpsJ092C	1.62	Middle Waste	mudstone	16.9 (6)	9.7 (4)	7 (1)	1.4 (8)	2.0 (6)	0.1 (8)	17 (1)	27.7 (9)	12.1 (7)	4.6 (3)
wpsJ091C	1.52	Middle Waste	mudstone	4.5 (4)	9.2 (3)	4.3 (7)	0.1 (6)	2.3 (6)	0.1 (7)	16 (1)	47 (1)	14.0 (6)	2.2 (2)
wpsJ086C	1.60	Middle Waste	dolostone	1.7 (3)	0.7 (1)	0.1 (1)	2 (5)	1.8 (4)	0.7 (5)	6.1 (7)	69 (1)	15.1 (4)	0.8 (1)
wpsJ084C	1.55	Middle Waste	carbon seam	41 (1)	12.0 (4)	18 (2)	2 (1)	0.6 (4)	0.1 (7)	6.3 (8)	2.7 (3)	10.0 (3)	5.4 (2)
wpsJ083C	1.79	Middle Waste	dolostone	33 (1)	14.6 (5)	10 (1)	0.1 (9)	1.8 (5)	0.1 (9)	20 (1)	4.4 (9)	8.5 (7)	6.8 (3)
wpsJ079C	1.46	Middle Waste	dolostone	4.7 (4)	3.9 (2)	1.6 (3)	0.1 (5)	0.8 (3)	0.0 (5)	7.4 (7)	66.2 (9)	13.3 (5)	1.9 (2)
wpsJ070C	2.23	Middle Waste	mudstone	11.3 (6)	27.5 (8)	11.1 (1)	1.5 (8)	12.8 (7)	0 (8)	16 (1)	9 (1)	3.7 (8)	4.0 (2)
wpsJ067C	1.90	Middle Waste	siltstone	17.0 (5)	9.6 (2)	6.2 (8)	0.1 (7)	5.7 (5)	0.0 (6)	7.1 (8)	25.3 (5)	26.5 (5)	2.5 (2)

Table 1a: (continued)

Sample	χ^2	Unit	Lithology	apatite	quartz	muscovite	illite	albite	orthoclase	buddingtonite	dolomite	calcite	pyrite
wpsJ065C	1.80	Middle Waste	mudstone	20.4 (7)	19.6 (6)	9 (1)	0.1 (9)	6.1 (7)	0.1 (9)	14 (1)	7.7 (5)	17.7 (6)	4.6 (3)
wpsJ063C	1.86	Middle Waste	mudstone	11.0 (5)	2.8 (2)	12 (1)	3.0 (7)	0.0 (5)	0.0 (7)	4.5 (9)	10.3 (8)	53 (1)	2.1 (2)
wpsJ061C	1.60	Middle Waste	mudstone	13.5 (6)	11.0 (3)	8 (1)	1.9 (7)	0.0 (6)	0.1 (7)	16.8 (9)	5.1 (2)	37.3 (9)	3.7 (2)
wpsJ059C	1.51	Middle Waste	mudstone	9.6 (6)	9.7 (4)	2.5 (9)	1.6 (9)	1.1 (7)	0.1 (9)	14 (1)	5.2 (3)	52 (1)	2.7 (3)
wpsJ057C	2.07	Middle Waste	mudstone	27.7 (1)	9.3 (4)	9.4 (5)	3.5 (8)	0.0 (8)	0 (1)	14 (1)	6.1 (4)	22.6 (9)	6.3 (3)
wpsJ054C	1.90	Middle Waste	mudstone	2.5 (7)	6.2 (3)	0.1 (8)	0.1 (7)	12.2 (6)	0.0 (8)	6 (1)	47 (1)	24.5 (6)	1.8 (2)
wpsJ052C	1.72	Middle Waste	mudstone	14.9 (5)	27.3 (6)	10 (1)	0.1 (5)	8.2 (5)	0.2 (6)	14.2 (9)	9.7 (2)	10.3 (3)	3.6 (2)
wpsJ050C	1.64	Middle Waste	mudstone	25.9 (7)	9.3 (3)	12 (1)	0.1 (6)	5.2 (6)	0.7 (7)	17 (1)	2.3 (2)	19.4 (5)	5.3 (2)
wpsJ048C	1.56	C Bed Ore	siltstone	46.1 (9)	5.3 (2)	3 (7)	0.1 (7)	1.7 (5)	0.9 (6)	5.6 (6)	26.7 (7)	6.3 (6)	3.2 (2)
wpsJ047C	1.58	C Bed Ore	phosphorite	58 (1)	6.4 (3)	11 (1)	0.3 (8)	2.0 (6)	1.0 (7)	8 (1)	3.9 (4)	4.6 (3)	4.1 (2)
wpsJ045C	1.50	C Bed Ore	phosphorite	60 (1)	5.3 (3)	5 (1)	0.1 (8)	0.1 (1)	0.9 (7)	1.4 (7)	19.4 (5)	5.3 (3)	1.7 (2)
wpsJ040C	1.60	C Bed Ore	phosphorite	78 (2)	2.7 (4)	0 (1)	1 (1)	5 (1)	0 (1)	0 (1)	0.0 (6)	10.4 (8)	0.9 (3)
wpsJ037C	1.48	C Bed Ore	phosphorite	33.5 (7)	5.6 (3)	2.3 (8)	0.1 (7)	2.1 (5)	0.7 (6)	0.3 (6)	50 (1)	4.7 (6)	0.8 (2)
wpsJ035C	1.60	C Bed Ore	phosphorite	54 (1)	14.4 (4)	5 (1)	0.1 (8)	6.3 (6)	6 (1)	0.5 (7)	2.7 (4)	7.0 (4)	2.0 (2)
wpsJ034C	1.66	False Cap	siltstone	18.3 (6)	34.1 (7)	5.0 (9)	0.1 (7)	14.6 (5)	8.7 (6)	1.8 (6)	10.1 (7)	3.3 (3)	3.4 (2)
wpsJ031C	1.55	B Bed Ore	phosphorite	63 (1)	13.7 (3)	8 (1)	0.1 (7)	4.6 (5)	2 (6)	0.1 (6)	2.4 (3)	0.5 (3)	2.3 (2)
wpsJ025C	1.50	Lower Waste	siltstone	1.4 (4)	7.4 (2)	2.9 (8)	0.1 (7)	1.2 (1)	6.5 (5)	0.1 (4)	64 (1)	14.5 (6)	1.3 (2)
wpsJ023C	1.44	B Bed Ore	phosphorite	69 (2)	17.4 (4)	2 (1)	0.4 (7)	0.3 (2)	0.6 (6)	0.9 (4)	4.4 (5)	0.0 (3)	3.0 (2)
wpsJ022C	1.57	Lower Waste	siltstone	5.4 (5)	11 (3)	2.5 (8)	0.1 (7)	1.1 (8)	6.0 (5)	0.6 (3)	64 (1)	6.2 (5)	2.3 (2)
wpsJ021C	1.81	Lower Waste	mudstone	38 (1)	12.0 (5)	4.3 (1)	0 (1)	6 (1)	1.8 (9)	0.6 (6)	5.5 (5)	5.4 (4)	2.2 (3)
wpsJ020C	1.57	Lower Waste	mudstone	49 (1)	20.7 (5)	3 (1)	0.1 (8)	5.3 (6)	4.0 (7)	2.8 (7)	9.9 (5)	2.2 (3)	2.6 (2)
wpsJ018C	1.54	B Bed Ore	phosphorite	60 (1)	14.4 (3)	7 (1)	1.9 (7)	2.4 (5)	2.3 (6)	0.8 (6)	5.8 (4)	2.2 (3)	2.8 (2)
wpsJ017C	1.67	B Bed Ore	dolostone	15.0 (6)	3.8 (2)	2 (1)	0.1 (9)	1.9 (6)	2.7 (7)	0.5 (7)	62 (1)	12.0 (4)	0.0 (2)
wpsJ014C	1.58	B Bed Ore	phosphorite	65 (2)	10.9 (4)	4 (1)	0.1 (9)	0.1 (6)	3.0 (9)	3 (1)	12.4 (9)	0.4 (3)	0.0 (2)
wpsJ011C	1.63	Cap Rock	mudstone	29.3 (6)	8.7 (3)	0.9 (3)	0.1 (7)	0.6 (5)	1.5 (6)	0.6 (6)	50.7 (8)	5.3 (3)	1.4 (2)

Table 1a: (continued)

Sample	χ^2	Unit	Lithology	apatite	quartz	muscovite	illite	albite	orthoclase	buddingtonite	dolomite	calcite	pyrite
wpsJ008C	1.54	A Bed Ore	phosphorite	86 (2)	5.3 (3)	7 (2)	0 (1)	0.1 (7)	0.1 (8)	0.1 (8)	0.4 (4)	0.0 (3)	0.2 (2)
wpsJ006C	1.68	Footwall	siltstone	24.7 (7)	42.7 (9)	8 (1)	2.5 (8)	0.0 (6)	2.2 (7)	0.6 (7)	7.3 (3)	1.0 (1)	5.1 (2)
wpsJ003C	1.87	Footwall	dolostone	0.0 (4)	19.0 (4)	5 (8)	0.1 (7)	0.0 (5)	3.0 (5)	0.9 (6)	69 (1)	3.2 (2)	0.0 (2)
wpsJ002C	1.91	Footwall	dolostone	1.4 (6)	50 (2)	21 (2)	1 (1)	0.0 (7)	1.6 (9)	2.5 (9)	15 (1)	4.1 (4)	0.0 (3)
wpsJ0.5C	1.40	Fish-scale bed	phosphorite	83 (3)	3.3 (3)	11 (3)	0 (1)	0.3 (7)	0.1 (8)	0 (1)	2.2 (3)	0.3 (3)	0.2 (3)
wpsJ-01C	1.44	Grandeur	dolostone	1.1 (4)	1.2 (2)	1.8 (9)	0.1 (8)	0.0 (5)	0.0 (6)	1.2 (6)	94 (2)	0.0 (3)	0.1 (2)
wpsJ-03C	1.79	Grandeur	dolostone	0.1 (3)	1.1 (5)	1.4 (8)	0.1 (8)	0.0 (5)	0.0 (5)	0.5 (6)	97 (2)	0.0 (3)	0.0 (2)
wpsJ-05C	1.61	Grandeur	dolostone	0.5 (3)	1.2 (3)	0.9 (4)	0.1 (6)	0.0 (5)	0.0 (6)	0.9 (4)	96 (2)	0.0 (2)	0.0 (2)

Table 1b: Quantitative mineralogy for section J individual samples calculated using the Rietveld method. The χ^2 value is a numerical statement of the quality of the match between the collected XRD pattern and the calculated Rietveld pattern where any value less than 3 is considered acceptable, with smaller χ^2 values inferring better results. Weight percents are listed with an accepted error in the last decimal place given in parentheses.

Sample	χ^2	Unit	Lithology	apatite	quartz	muscovite	illite	albite	orthoclase	buddingtonite	dolomite	calcite	pyrite
wpsJ188.2K	1.53	Rex Chert	chert	39 (1)	43 (1)	12 (2)	3.1 (9)	0.1 (7)	0.1 (7)	0.1 (8)	0.0 (3)	0.0 (3)	0.9 (2)
wpsJ186.8K	2.67	Upper Waste	phosphorite	56 (1)	26.5 (5)	4.8 (7)	2.4 (8)	0.0 (6)	0.3 (6)	1.3 (7)	0.0 (2)	0.0 (3)	4.4 (4)
wpsJ186.2K	1.52	Upper Waste	phosphorite	71 (2)	14.6 (5)	6 (2)	1.5 (8)	0.1 (6)	0.1 (7)	0.1 (7)	0.0 (2)	0.0 (3)	4.2 (3)
wpsJ185.9K	1.42	Upper Waste	phosphorite	71 (1)	18.2 (4)	4 (1)	3.4 (7)	0.1 (6)	0.1 (6)	1.2 (7)	0.0 (2)	0.0 (3)	1.4 (2)
wpsJ185.2K	1.48	Upper Waste	phosphorite	76 (1)	10.8 (3)	8 (1)	0.1 (7)	0.0 (2)	0.1 (5)	0.1 (6)	0.1 (2)	0.0 (2)	2.1 (2)
wpsJ175.7K	1.89	Upper Waste	mudstone	8.8 (7)	40 (1)	25 (2)	2 (1)	6.7 (7)	0.3 (8)	1.2 (9)	9 (1)	0.0 (4)	5.9 (4)
wpsJ174.7K	1.84	Upper Waste	mudstone	15.7 (7)	44 (1)	19 (1)	1.5 (9)	6.8 (8)	0.0 (7)	0.5 (8)	6 (1)	0.0 (3)	5.4 (3)
wpsJ170.3K	1.81	Upper Waste	mudstone	36.2 (9)	29.8 (7)	15 (1)	2.8 (9)	8.0 (7)	0.1 (7)	0.7 (8)	0.0 (4)	0.0 (3)	2.1 (2)
wpsJ162.4K	1.44	Upper Ore	phosphorite	89 (2)	3.2 (3)	6.8 (2)	0.3 (8)	0.1 (5)	0.1 (6)	0.1 (7)	0.0 (3)	0.0 (3)	0.0 (2)
wpsJ161.8K	1.50	Upper Ore	phosphorite	78 (2)	4.7 (2)	16 (2)	0.1 (8)	0.0 (6)	0.4 (6)	0.0 (7)	0.0 (3)	0.0 (3)	0.0 (2)
wpsJ152.2K	1.51	Upper Ore	phosphorite	66 (2)	12.8 (4)	15 (2)	0.5 (9)	3.1 (6)	0.1 (7)	0.1 (7)	0.0 (4)	0.0 (3)	0.9 (2)
wpsJ150.5K	1.78	Upper Ore	phosphorite	72 (2)	7.7 (3)	5 (1)	0 (1)	13.3 (7)	0.1 (7)	0.3 (8)	0.0 (4)	0.2 (3)	0.0 (2)
wpsJ146.2K	1.62	Middle Waste	mudstone	39.2 (9)	34.4 (8)	6 (1)	2.8 (8)	2.0 (7)	1.7 (7)	9.7 (8)	0.0 (4)	0.0 (3)	1.5 (2)
wpsJ141.1K	1.67	Middle Waste	dolostone	22.7 (6)	41.3 (9)	7 (1)	0.3 (8)	8.0 (5)	2.6 (6)	10.9 (8)	0.0 (3)	0.0 (3)	5.5 (2)
wpsJ140.1K	1.70	Middle Waste	mudstone	30 (1)	35 (1)	14 (2)	0.8 (9)	1.4 (7)	0.7 (8)	10.9 (8)	0.0 (4)	0.0 (3)	4.3 (3)
wpsJ139.8K	1.89	Middle Waste	mudstone	24.1 (8)	40 (1)	14 (1)	0.1 (9)	2.6 (6)	0.0 (8)	12 (1)	0.0 (4)	0.0 (3)	2.8 (2)
wpsJ138.6K	1.58	Middle Waste	mudstone	33.4 (8)	35.4 (8)	11 (1)	1.0 (8)	1.8 (6)	0.1 (6)	11.4 (6)	0.0 (3)	0.0 (3)	3.6 (2)
wpsJ138.4K	1.67	Middle Waste	mudstone	49 (1)	24.9 (5)	5.2 (9)	0.1 (9)	6.2 (6)	2.5 (7)	4.6 (7)	0.4 (4)	0.0 (3)	2.9 (2)
wpsJ138.2K	1.63	Middle Waste	mudstone	47 (1)	30.1 (9)	5 (1)	0.9 (9)	0.1 (7)	2.7 (8)	8 (1)	0.0 (4)	0.0 (3)	3.0 (3)
wpsJ137.3K	1.48	Middle Waste	mudstone	72 (2)	16.1 (4)	0.1 (7)	3.3 (5)	0.7 (6)	2.1 (6)	2.2 (3)	0.1 (3)	0.1 (3)	0.8 (2)
wpsJ137.1K	2.14	Middle Waste	mudstone	14.3 (7)	28.0 (8)	17 (2)	2.9 (8)	7.7 (6)	3.3 (8)	9 (1)	6.7 (5)	0.0 (3)	5.3 (2)
wpsJ136.8K	2.04	Middle Waste	dolostone	20.3 (7)	37.7 (9)	13 (1)	0.1 (9)	10.6 (6)	0.1 (8)	8.5 (8)	3.1 (9)	0.0 (3)	5.8 (3)
wpsJ136.4K	1.71	Middle Waste	mudstone	49 (2)	14.7 (5)	21 (2)	0.1 (8)	2.1 (6)	0.7 (7)	2.9 (7)	0.0 (3)	0.0 (3)	4.1 (2)
wpsJ135.7K	1.60	Middle Waste	mudstone	67 (1)	11.8 (3)	6 (1)	0.1 (8)	7.2 (6)	0.1 (7)	1.8 (7)	2.7 (4)	0.2 (3)	2.0 (2)
wpsJ135.4K	1.52	Middle Waste	mudstone	60 (1)	20.2 (5)	3 (1)	0.1 (8)	3.9 (6)	0.8 (7)	4.3 (6)	3.7 (3)	0.0 (3)	2.4 (2)

Table 1b: (continued)

Sample	χ^2	Unit	Lithology	apatite	quartz	muscovite	illite	albite	orthoclase	buddingtonite	dolomite	calcite	pyrite
wpsJ135.2K	1.66	Middle Waste	mudstone	29.3 (7)	31.5 (6)	12 (1)	1.1 (7)	7.3 (6)	3.2 (6)	4.3 (6)	3.8 (3)	0.0 (3)	6.1 (2)
wpsJ135.0K	1.81	Middle Waste	mudstone	18.1 (7)	43 (1)	4 (1)	0.1 (9)	12.9 (7)	1.2 (7)	7.3 (8)	5.9 (9)	0.0 (3)	5.2 (3)
wpsJ127.7K	1.62	Middle Waste	siltstone	0.4 (4)	17.6 (3)	2.5 (6)	0.1 (7)	8.4 (5)	0.0 (5)	6.4 (5)	55.4 (9)	3.6 (2)	2.6 (2)
wpsJ117.6K	1.51	Middle Waste	mudstone	59 (1)	19.3 (4)	6 (1)	0.1 (7)	2.9 (5)	1.1 (5)	7.2 (36)	0.0 (3)	0.2 (2)	1.9 (2)
wpsJ109.9K	1.62	Middle Waste	phosphorite	2.8 (3)	35.5 (7)	1.8 (7)	0.1 (6)	12.3 (5)	0.0 (6)	19 (8)	24.7 (7)	0.0 (2)	3.3 (2)
wpsJ107.9K	1.53	Middle Waste	phosphorite	62 (2)	15.6 (4)	6 (1)	0.4 (9)	3.0 (7)	0.1 (7)	6 (1)	1.3 (4)	0 (3)	2.3 (2)
wpsJ105.8K	1.69	Middle Waste	mudstone	26.9 (9)	27.5 (8)	12 (1)	0.1 (9)	5.5 (6)	0.1 (8)	15 (1)	3.0 (8)	2.5 (9)	4.9 (3)
wpsJ105.4K	1.76	Middle Waste	mudstone	16.4 (7)	26.4 (8)	18 (2)	1.5 (9)	0.4 (6)	0.1 (7)	8.4 (8)	3.3 (9)	15.7 (7)	5.9 (4)
wpsJ104.9K	1.72	Middle Waste	mudstone	0.0 (6)	53 (1)	2.3 (1)	0 (1)	10.2 (9)	0.2 (9)	23 (1)	3.9 (9)	4.7 (9)	2.3 (3)
wpsJ103.3K	1.54	Middle Waste	mudstone	44 (1)	11.2 (6)	7 (1)	0 (1)	0.0 (1)	0 (1)	3 (1)	1.0 (1)	27 (1)	2.7 (4)
wpsJ97.2K	1.44	Middle Waste	dolostone	2.5 (3)	1.8 (2)	0.1 (7)	0.1 (6)	0.7 (4)	0.1 (4)	2.1 (5)	71 (1)	20.4 (6)	1.0 (2)
wpsJ96.5K	1.65	Middle Waste	carbon seam	26.7 (8)	14.6 (4)	13 (1)	0.1 (8)	0.7 (6)	0.1 (7)	17 (1)	12.9 (8)	5.8 (6)	5.9 (3)
wpsJ96.4K	1.47	Middle Waste	dolostone	0.0 (3)	2.6 (1)	1.2 (7)	0.1 (6)	0.7 (4)	1.5 (4)	6.7 (6)	57.5 (9)	27.4 (6)	1.6 (1)
wpsJ95.4K	1.61	Middle Waste	carbon seam	35 (1)	17.8 (6)	6 (1)	0.1 (9)	2.6 (7)	0.3 (7)	11 (1)	2.8 (9)	17.8 (9)	4.8 (3)
wpsJ95.3K	1.36	Middle Waste	dolostone	1.1 (3)	1.5 (2)	0.1 (7)	2.0 (6)	0.0 (4)	0.1 (4)	0.0 (5)	14.2 (6)	81 (1)	0.0 (2)
wpsJ94.9K	1.65	Middle Waste	mudstone	30.0 (9)	19.8 (6)	15 (1)	1.5 (9)	1.9 (7)	2.2 (7)	8.7 (9)	4.7 (9)	7.5 (7)	8.0 (4)
wpsJ94.0K	1.60	Middle Waste	mudstone	34 (1)	17.9 (6)	12 (1)	0 (1)	3.7 (7)	0.1 (8)	12 (1)	2.9 (9)	8.2 (8)	6.4 (4)
wpsJ93.8K	1.75	Middle Waste	mudstone	34 (1)	23 (1)	6 (1)	3 (1)	0.1 (8)	0.1 (8)	12 (1)	2 (1)	11 (1)	5.7 (4)
wpsJ93.4K	1.76	Middle Waste	mudstone	13.4 (7)	21.0 (7)	11 (1)	0 (1)	1.0 (7)	3.3 (8)	33 (1)	6 (1)	3.7 (7)	7.1 (4)
wpsJ93.13K	1.37	Middle Waste	dolostone	0.0 (3)	2 (1)	0.1 (1)	0.1 (5)	2.0 (4)	0.9 (4)	4.7 (4)	69.8 (8)	18.4 (4)	1.1 (1)
wpsJ85.1K	1.45	Middle Waste	dolostone	1.0 (4)	2.2 (2)	0.1 (8)	0.1 (7)	0.4 (5)	0.5 (5)	3.2 (9)	75 (1)	15.9 (5)	1.0 (2)
wpsJ84.7K	1.31	Middle Waste	dolostone	1.1 (3)	1.2 (2)	0.3 (7)	0.1 (6)	0.6 (4)	0.7 (5)	4.6 (8)	73 (1)	17.5 (5)	0.4 (2)
wpsJ83.8K	1.71	Middle Waste	carbon seam	35 (1)	15.2 (7)	20 (2)	2 (1)	0.1 (9)	0 (1)	8 (1)	3 (1)	4.5 (9)	9.3 (6)
wpsJ83.57K	1.59	Middle Waste	mudstone	50 (1)	11.6 (4)	10 (1)	0.1 (9)	0.1 (7)	0.1 (7)	8 (1)	5.0 (4)	8.7 (7)	5.5 (4)
wpsJ82.53K	1.70	Middle Waste	mudstone	31.0 (9)	21.7 (6)	11 (1)	0.1 (9)	2.3 (7)	0.4 (7)	11.3 (1)	5 (1)	7.9 (7)	7.6 (3)

Table 1b: (continued)

Sample #	χ^2	Unit	Lithology	apatite	quartz	muscovite	illite	albite	orthoclase	buddingtonite	dolomite	calcite	pyrite
wpsJ82.33K	1.81	Middle Waste	mudstone	10.1 (6)	24.1 (6)	13 (1)	0.1 (8)	12.5 (6)	0.1 (7)	14.0 (9)	7.1 (9)	7.2 (7)	8.9 (4)
wpsJ82.27K	1.66	Middle Waste	mudstone	32.9 (9)	15.9 (4)	16 (1)	0.5 (8)	2.4 (6)	0.1 (7)	15 (1)	6.6 (5)	2.7 (3)	6.6 (3)
wpsJ82.2K	1.79	Middle Waste	mudstone	15.6 (7)	23.5 (7)	15 (1)	0.1 (9)	7.1 (7)	0.1 (8)	19 (1)	5 (9)	1.8 (7)	8.4 (4)
wpsJ82.1K	1.61	Middle Waste	mudstone	33.8 (9)	12.5 (4)	18 (1)	0.1 (8)	0.0 (6)	0.1 (6)	13.7 (9)	5.3 (8)	7.6 (6)	6.9 (3)
wpsJ82.07K	1.75	Middle Waste	dolostone	19.8 (8)	18.0 (6)	15 (2)	0 (1)	0.7 (7)	0.1 (8)	25 (1)	5.6 (9)	5.7 (7)	7.7 (4)
wpsJ81.7K	1.69	Middle Waste	dolostone	19.4 (6)	10.4 (3)	16 (1)	0.1 (8)	0.0 (6)	0.9 (6)	15.1 (9)	8.6 (4)	21.9 (7)	5.9 (3)
wpsJ81.1K	1.51	Middle Waste	dolostone	1.4 (3)	2.2 (2)	0.4 (8)	0.4 (7)	1.3 (5)	0.7 (5)	3.8 (5)	73 (1)	15.1 (5)	0.8 (2)
wpsJ75.2K	1.95	Middle Waste	mudstone	7.7 (5)	32.1 (7)	11.3 (9)	0.1 (7)	10.5 (6)	3.2 (6)	19.5 (8)	7.0 (7)	0.8 (3)	5.3 (3)
wpsJ73.3K	1.67	Middle Waste	mudstone	17.8 (7)	23.6 (6)	14 (1)	0.1 (8)	2.8 (6)	0.1 (8)	16 (1)	6.7 (8)	9.0 (6)	8.4 (3)
wpsJ68.1K	1.67	Middle Waste	mudstone	42.8 (9)	13.8 (3)	11.1 (9)	0.1 (8)	4.2 (5)	0.1 (7)	18.5 (9)	3.8 (3)	0.5 (3)	3.2 (2)
wpsJ62.7K	1.50	Middle Waste	mudstone	11.9 (5)	12.1 (3)	5 (1)	0.7 (7)	1.3 (5)	0.6 (6)	8.5 (8)	7.5 (7)	48 (1)	3.2 (2)
wpsJ56.0K	1.69	Middle Waste	mudstone	12.9 (6)	12.4 (4)	10 (1)	0.1 (9)	4.4 (7)	0.1 (9)	20 (1)	7.5 (9)	26 (1)	6.5 (4)
wpsJ50.8K	1.89	Middle Waste	mudstone	6.2 (6)	13.2 (5)	18 (1)	0.1 (9)	3.5 (7)	0.1 (9)	28 (1)	5.4 (9)	12.6 (8)	8.3 (4)
wpsJ36.6K	1.65	Lower Ore	phosphorite	73 (2)	8.6 (3)	3 (1)	0 (1)	0.0 (7)	2.2 (8)	1.4 (8)	6.7 (6)	1.2 (3)	2.5 (3)
wpsJ36.2K	1.42	Lower Ore	phosphorite	80 (2)	6.4 (3)	4 (1)	0 (1)	2.6 (7)	0.2 (8)	0.5 (8)	2 (1)	0.3 (3)	1.9 (3)
wpsJ35.7K	1.52	Lower Ore	phosphorite	65 (1)	14.3 (3)	3.4 (4)	0.1 (7)	3.7 (5)	1.6 (7)	0.9 (7)	4.2 (3)	1.9 (3)	3.4 (2)
wpsJ27.0K	1.48	Lower Ore	phosphorite	88 (2)	4.7 (3)	5 (2)	0.1 (9)	0.6 (6)	0.1 (7)	0.3 (7)	0.0 (4)	0.0 (3)	0.9 (2)
wpsJ18.8K	1.65	Lower Ore	phosphorite	55 (1)	20.9 (6)	9 (1)	0.1 (9)	2.6 (6)	1.0 (7)	1.3 (7)	2.0 (1)	0.0 (3)	6.4 (3)
wpsJ8.8K	1.56	Lower Ore	phosphorite	82 (2)	4.6 (3)	2 (2)	0.6 (8)	0.1 (6)	0.1 (7)	0.3 (7)	4.3 (4)	0.0 (3)	1.1 (2)
wpsJ8.7K	1.47	Lower Ore	phosphorite	83 (2)	3.5 (2)	11 (2)	0.1 (8)	0.1 (6)	0.1 (6)	0.1 (7)	0.8 (3)	0.0 (3)	0.8 (2)
wpsJ8.6K	1.55	Lower Ore	phosphorite	75 (2)	3.0 (2)	19 (2)	0.1 (8)	0.0 (6)	0.1 (6)	0.0 (6)	0.5 (3)	0.0 (3)	0.7 (2)
wpsJ8.3K	1.48	Lower Ore	siltstone	89 (2)	4.2 (3)	0.8 (2)	0.1 (9)	0.1 (7)	0.1 (7)	0.2 (8)	2.5 (4)	0.0 (3)	0.5 (3)
wpsJ8.2K	1.52	Lower Ore	siltstone	75 (2)	4.4 (3)	13 (2)	0.1 (8)	0.1 (6)	0.1 (7)	2.9 (4)	0.0 (3)	0.0 (3)	2.2 (3)
wpsJ8.0K	1.61	Lower Ore	siltstone	80 (2)	7.1 (3)	7 (2)	0 (1)	0.1 (8)	0.1 (7)	0.9 (8)	2.3 (5)	0.0 (4)	1.2 (3)
wpsJ7.6K	1.59	Lower Ore	siltstone	80 (2)	6.6 (3)	7 (1)	0.1 (8)	0.1 (6)	0.1 (6)	0.1 (7)	1.1 (4)	0.0 (3)	1.5 (32)

Table 1b: (continued)

Sample #	χ^2	Unit	Lithology	apatite	quartz	muscovite	illite	albite	orthoclase	buddingtonite	dolomite	calcite	pyrite
wpsJ7.3K	1.42	Lower Ore	siltstone	0.3 (4)	1.8 (2)	2.5 (9)	0.1 (8)	0.2 (5)	0.0 (6)	0.0 (6)	93 (2)	0.1 (3)	0.6 (2)
wpsJ5.4K	1.88	Lower Ore	siltstone	1.4 (4)	54 (1)	9 (1)	2 (8)	0.5 (6)	5.9 (7)	0.7 (7)	10.8 (9)	2.6 (3)	5.9 (3)
wpsJ2.85K	1.79	Lower Ore	dolostone	0.0 (4)	20.4 (4)	4.6 (9)	0.1 (7)	3.1 (5)	3.5 (6)	0.6 (6)	60 (1)	6.8 (3)	0.0 (2)
wpsJ1.89K	1.77	Lower Ore	dolostone	0.0 (6)	69 (2)	15 (1)	0 (1)	0.0 (9)	1 (1)	0 (1)	9 (1)	1.4 (4)	0.5 (2)
wpsJ1.6K	1.70	Lower Ore	dolostone	1.2 (7)	64 (2)	11 (1)	0 (1)	0.1 (8)	3.5 (9)	0.1 (8)	15 (1)	0.4 (4)	0.0 (3)
wpsJ1.26K	1.76	Lower Ore	dolostone	0.1 (6)	77 (2)	5 (1)	2 (1)	0.0 (7)	7 (1)	3.8 (9)	0.0 (5)	0.4 (4)	0.0 (3)
wpsJ0.8K	1.75	Lower Ore	dolostone	0.2 (6)	46 (2)	9 (1)	2.0 (9)	0.0 (8)	5.9 (8)	1.0 (8)	0.2 (1)	0.4 (4)	0.7 (3)
wpsJ0.2K	1.67	Lower Ore	phosphorite	76 (1)	3.3 (3)	3.2 (1)	0.1 (9)	0.1 (6)	0.1 (7)	0.3 (7)	15.9 (4)	0.3 (3)	0.1 (2)
wpsJ-3.2K	1.44	Grandeur	dolostone	1.5 (4)	2.9 (3)	2.4 (9)	0.1 (8)	1.2 (6)	1.4 (6)	0.6 (5)	89 (2)	0.3 (3)	0.2 (2)
wpsJ-6.5K	2.04	Grandeur	dolostone	0.0 (8)	5.7 (4)	2.0 (2)	0 (1)	1 (1)	4 (1)	0 (1)	89 (3)	0.0 (5)	0.3 (4)

Figure 3a: Apatite content of samples from the central part of Rasmussen Ridge, including the measured stratigraphic sections J (including channel and individual samples), B, and A. These sections represent respectively, least-weathered, less-weathered, and more-weathered strata of the Meade Peak Phosphatic Shale. Due to a lack of stratigraphic continuity, the three sections cannot be directly compared unit-to-unit, however, the recognized ore and waste zone boundaries are shown for reference. Section A and B data are from Knudsen and others (2000).

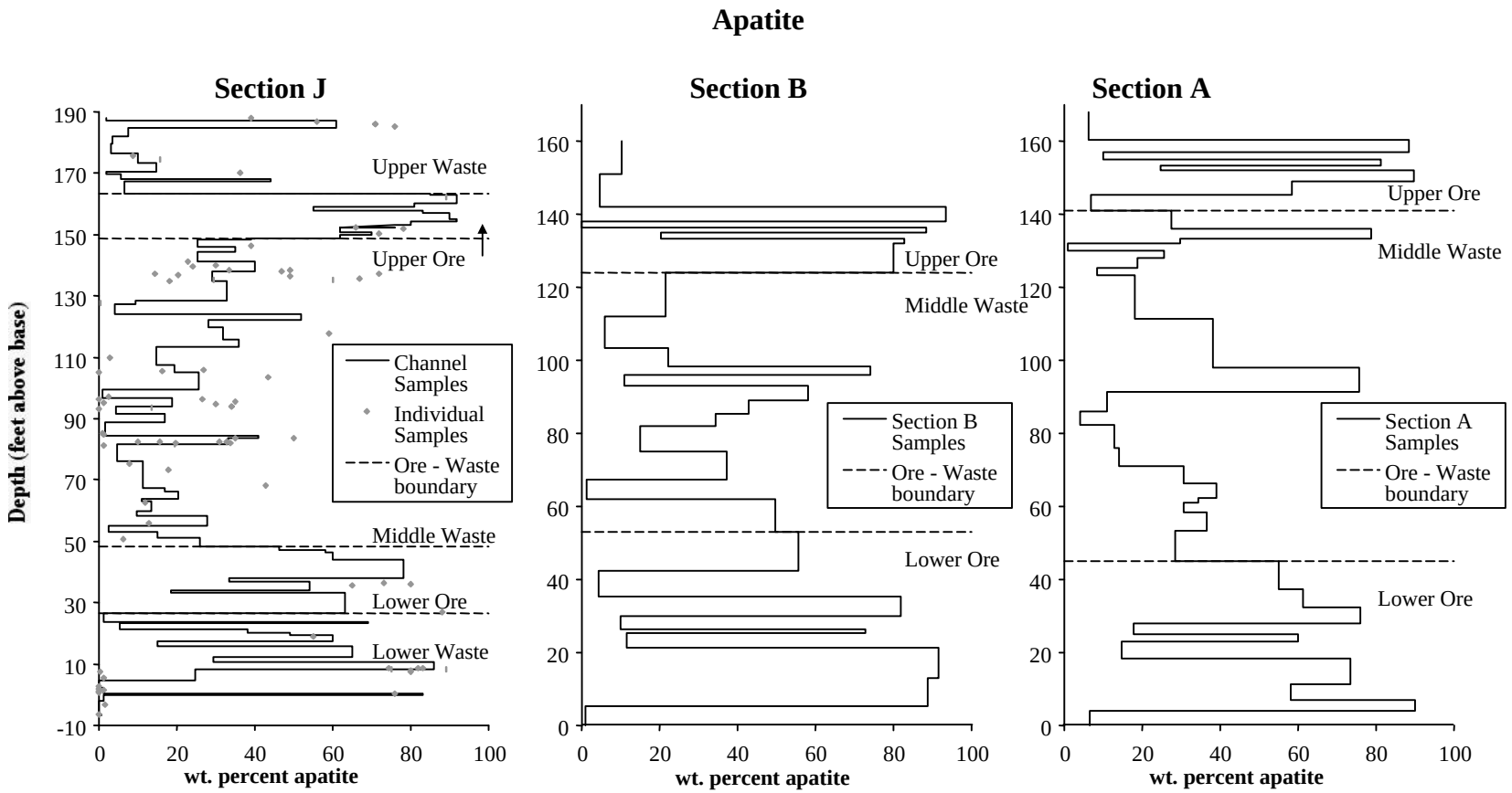

Figure 3b: Quartz content of samples from the central part of Rasmussen Ridge, including the measured stratigraphic sections J (including channel and individual samples), B, and A. These sections represent respectively, least-weathered, less-weathered, and more-weathered strata of the Meade Peak Phosphatic Shale. Due to a lack of stratigraphic continuity, the three sections cannot be directly compared unit-to-unit, however, the recognized ore and waste zone boundaries are shown for a point of reference. Section A and B data are from Knudsen and others (2000).

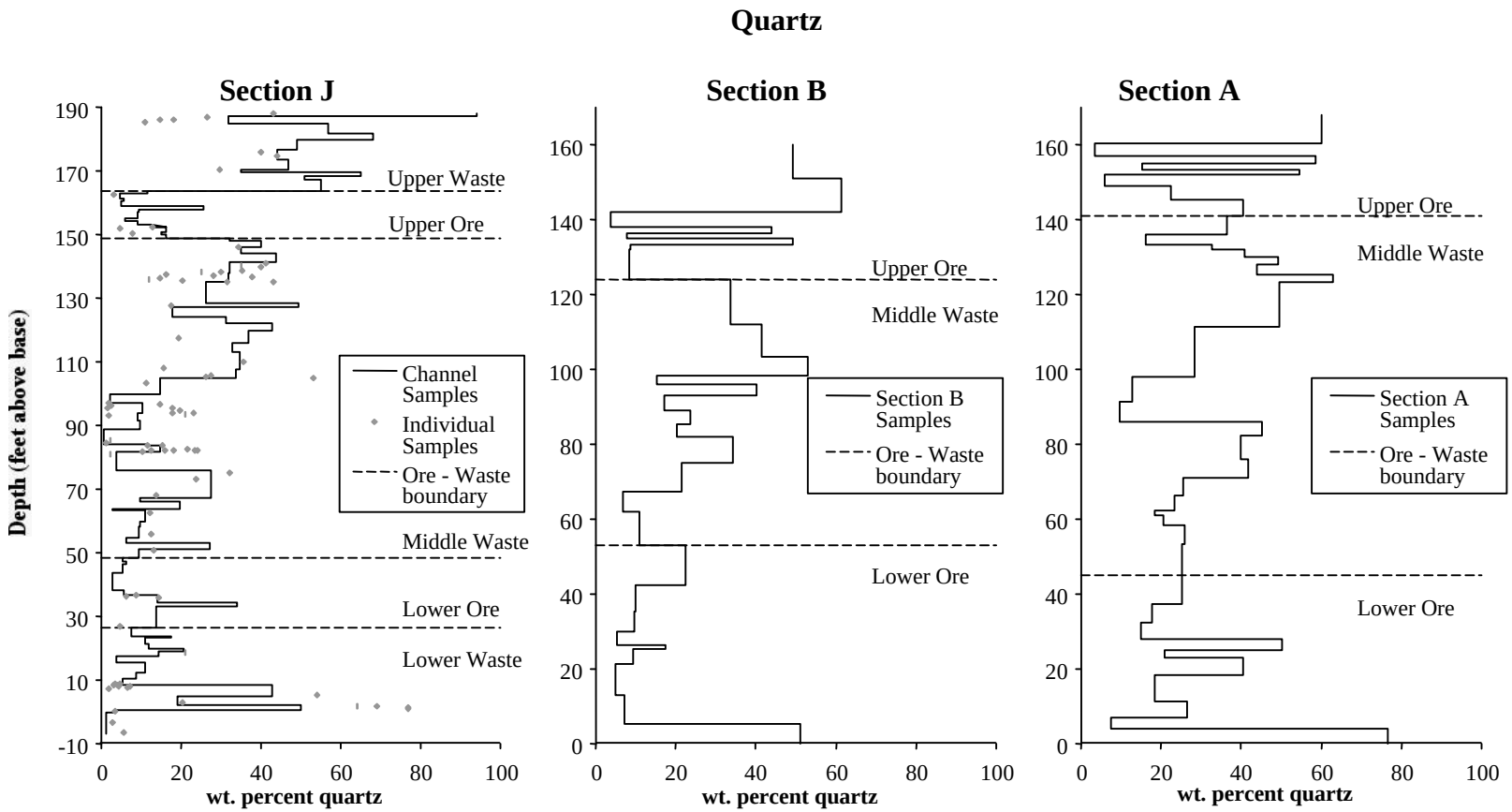

Figure 3c: Muscovite + illite content of samples from the central part of Rasmussen Ridge, including the measured stratigraphic sections J (including channel and individual samples), B, and A. These sections represent respectively, least-weathered, less-weathered, and more-weathered strata of the Meade Peak Phosphatic Shale. Due to a lack of stratigraphic continuity, the three sections cannot be directly compared unit-to-unit, however, the recognized ore and waste zone boundaries are shown for reference. Section A and B data are from Knudsen and others (2000).

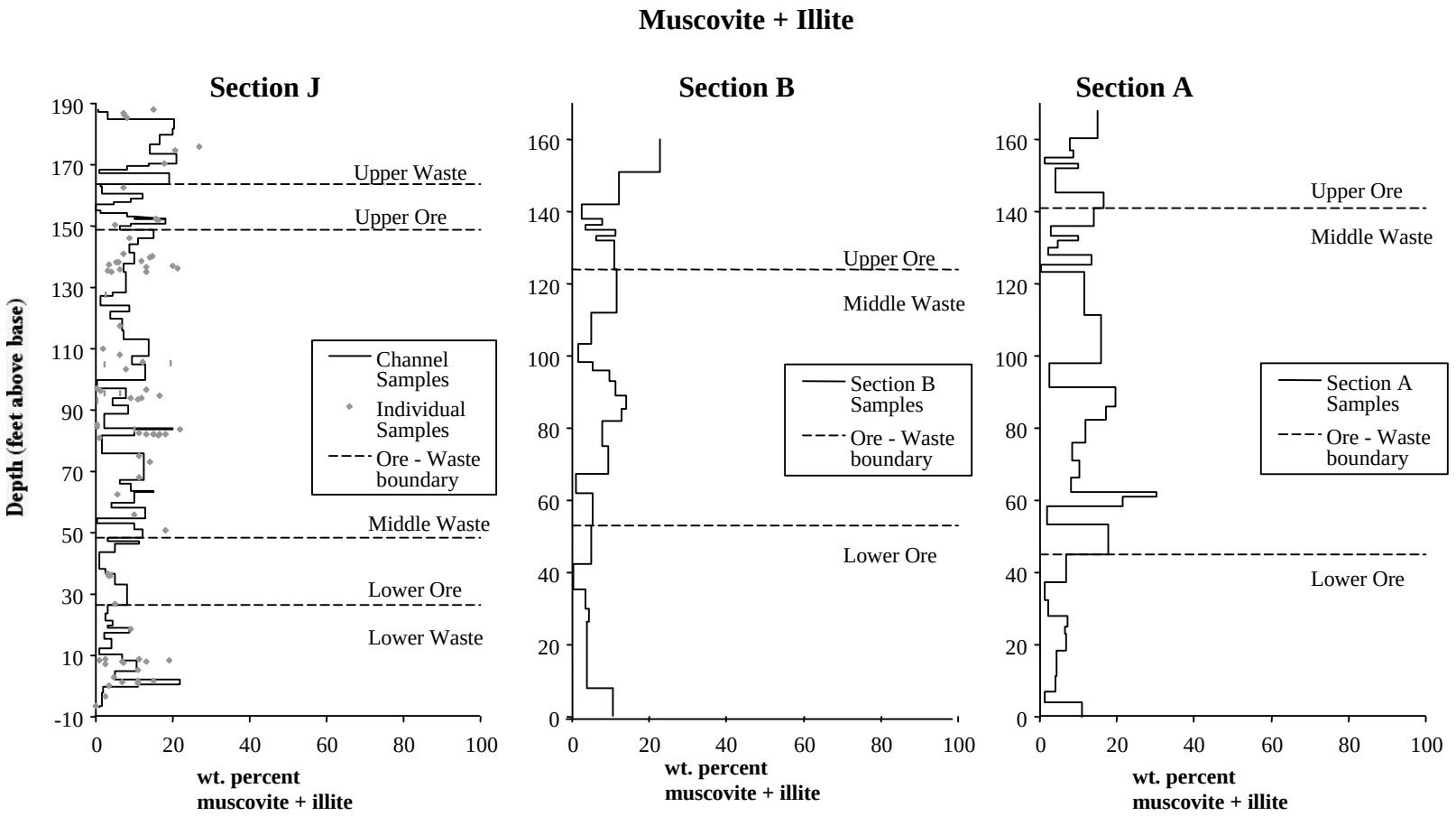

Figure 3d: Total feldspar (albite + orthoclase + buddingtonite) content of samples from the central part of Rasmussen Ridge, including the measured stratigraphic sections J (including channel and individual samples), B, and A. These sections represent respectively, least-weathered, less-weathered, and more-weathered strata of the Meade Peak Phosphatic Shale. Due to a lack of stratigraphic continuity, the three sections cannot be directly compared unit-to-unit, however, the recognized ore and waste zone boundaries are shown for reference. Section A and B data are from Knudsen and others (2000).

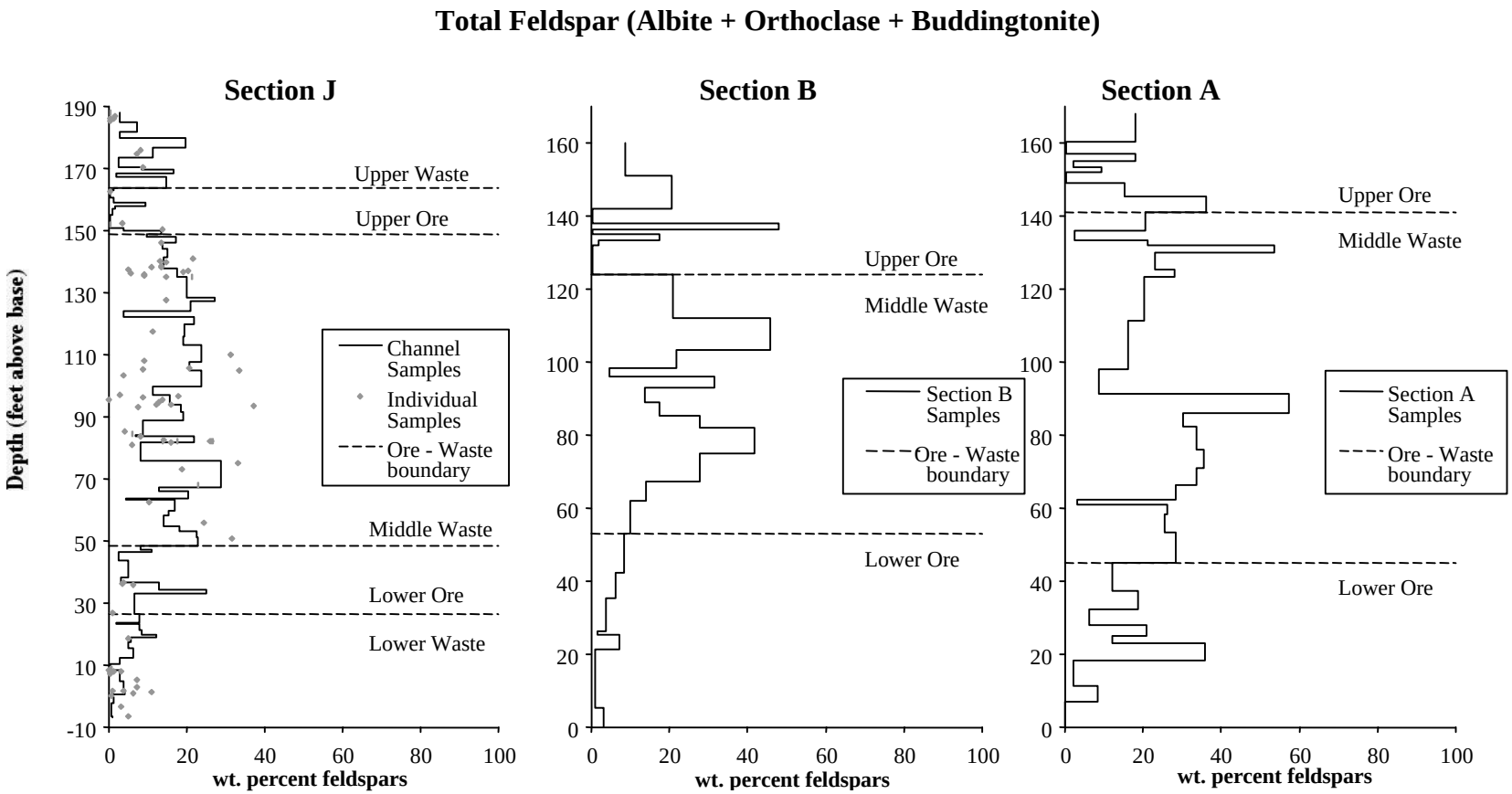

Figure 3e: Buddingtonite content of samples from the central part of Rasmussen Ridge, including the measured stratigraphic sections J (including channel and individual samples), B, and A. These sections represent respectively, least-weathered, less-weathered, and more-weathered strata of the Meade Peak Phosphatic Shale. Due to a lack of stratigraphic continuity, the three sections cannot be directly compared unit-to-unit, however, the recognized ore and waste zone boundaries are shown for reference. Section A and B data are from Knudsen and others (2000).

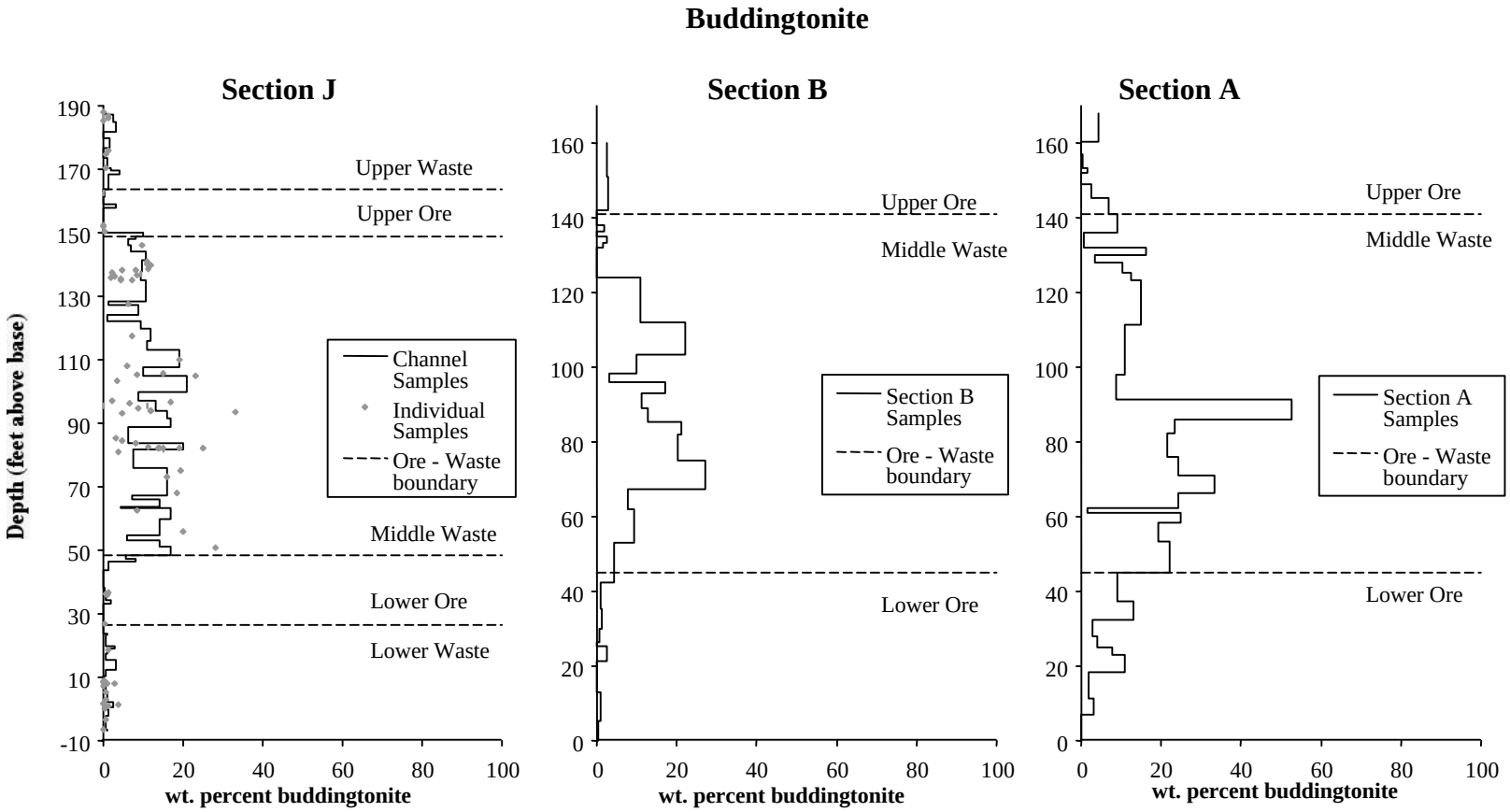

Figure 3f: Dolomite content of samples from the central part of Rasmussen Ridge, including the measured stratigraphic sections J (including channel and individual samples), B, and A. These sections represent respectively, least-weathered, less-weathered, and more-weathered strata of the Meade Peak Phosphatic Shale. Due to a lack of stratigraphic continuity, the three sections cannot be directly compared unit-to-unit, however, the recognized ore and waste zone boundaries are shown for reference. Section A and B data are from Knudsen and others (2000).

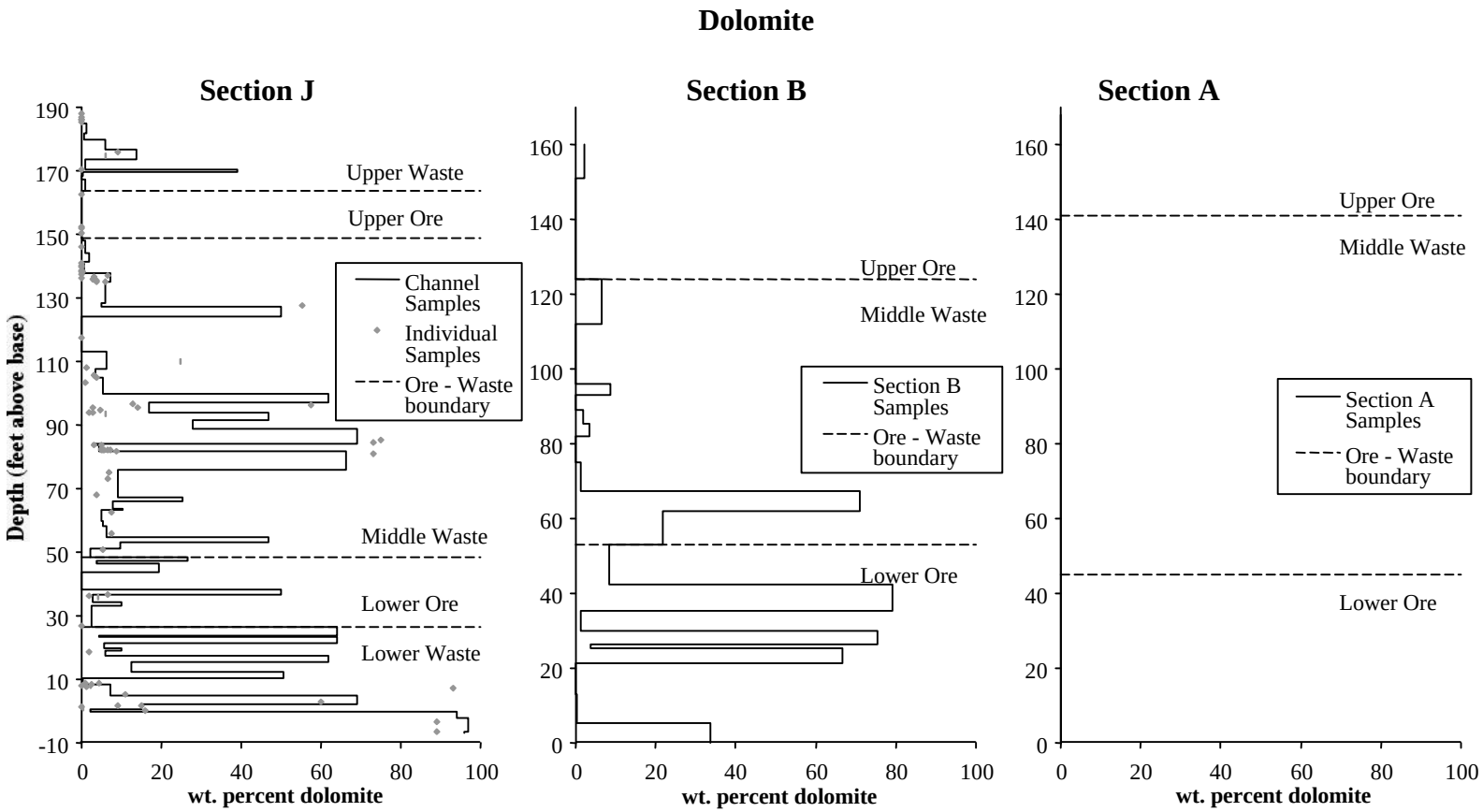

Figure 3g: Calcite content of samples from the central part of Rasmussen Ridge, including the measured stratigraphic sections J (including channel and individual samples), B, and A. These sections represent respectively, least-weathered, less-weathered, and more-weathered strata of the Meade Peak Phosphatic Shale. Due to a lack of stratigraphic continuity, the three sections cannot be directly compared unit-to-unit, however, the recognized ore and waste zone boundaries are shown for reference. Section A and B data are from Knudsen and others (2000).

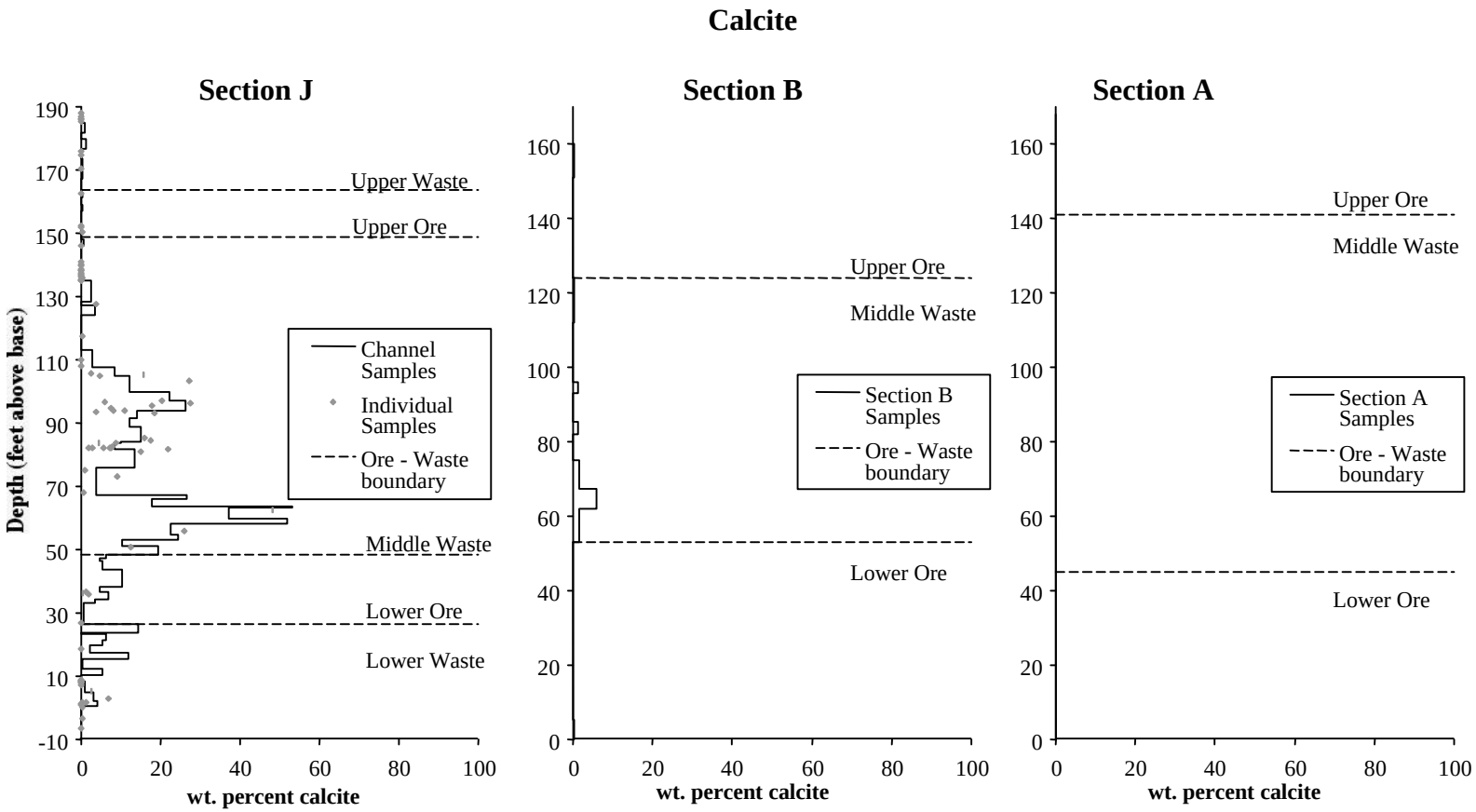

Table 2a: Data for CO_3^{2-} substitution in fluorapatite for section J channel samples based on the equation by Schuffert and others (1990):

$$y = 10.643x^2 - 52.512x + 56.986$$

Where y = the wt. % CO_3^{2-}, and x = $\Delta 2\theta_{(004)-(410)}$ for fluorapatite, as calculated by cell parameters obtained from Rietveld analysis.

WUSP Sample	Unit	Lithology	% apatite	CO_3^{2-} (wt %)
wpsJ187C	Rex Chert	chert	2	0.0
wpsJ186C	Upper Waste	phosphorite	61	2.5
wpsJ184C	Upper Waste	mudstone	8	0.0
wpsj181C	Upper Waste	mudstone	3	0.0
wpsJ177C	Upper Waste	mudstone	3	0.0
wpsJ175C	Upper Waste	mudstone	10	1.1
wpsJ172C	Upper Waste	mudstone	15	0.0
wpsJ170C	Upper Waste	mudstone	2	3.1
wpsJ169C	Upper Waste	siltstone	6	1.4
wpsJ168C	Upper Waste	phosphorite	44	2.2
wpsJ164C	Upper Waste	mudstone	7	0.5
wpsJ163C	Upper Ore	phosphorite	85	2.4
wpsJ162C	Upper Ore	phosphorite	92	2.5
wpsJ161C	Upper Ore	phosphorite	92	2.5
wpsJ160C	Upper Ore	phosphorite	81	2.5
wpsJ159C	Upper Ore	phosphorite	55	2.6
wpsJ158C	Upper Ore	phosphorite	83	2.6
wpsJ156C	Upper Ore	phosphorite	90	2.7
wpsJ155C	Upper Ore	phosphorite	92	3.0
wpsJ154C	Upper Ore	phosphorite	80	2.6
wpsJ153C	Upper Ore	phosphorite	76	2.7
wpsJ151C	Upper Ore	phosphorite	62	2.3
wpsJ150C	Upper Ore	phosphorite	70	2.6
wpsJ149C	Upper Ore	phosphorite	62	2.6
wpsJ148C	Middle Waste	siltstone	39	2.1
wpsJ147C	Middle Waste	mudstone	25	1.8
wpsJ145C	Middle Waste	siltstone	35	2.5
wpsJ143C	Middle Waste	siltstone	25	2.2
wpsJ140C	Middle Waste	mudstone	40	2.1
wpsJ136C	Middle Waste	mudstone	29	2.2
wpsJ131C	Middle Waste	siltstone	33	2.1
wpsJ128C	Middle Waste	siltstone	9	0.0
wpsJ125C	Middle Waste	mudstone	4	1.5
wpsJ123C	Middle Waste	mudstone	52	2.5
wpsJ121C	Middle Waste	mudstone	28	1.9
wpsJ117C	Middle Waste	mudstone	32	2.3
wpsJ114C	Middle Waste	mudstone	36	2.4
wpsJ111C	Middle Waste	phosphorite	15	1.0
wpsJ106C	Middle Waste	mudstone	19	2.1
wpsJ102C	Middle Waste	mudstone	26	2.5

Table 2a: (continued)

WUSP Sample	Unit	Lithology	% apatite	CO_3^{2-} (wt %)
wpsJ098C	Middle Waste	dolostone	1	0.0
wpsJ095C	Middle Waste	mudstone	19	2.6
wpsJ092C	Middle Waste	mudstone	5	2.3
wpsJ091C	Middle Waste	mudstone	17	0.0
wpsJ086C	Middle Waste	dolostone	2	0.0
wpsJ084C	Middle Waste	carbon seam	41	2.2
wpsJ083C	Middle Waste	dolostone	33	2.1
wpsJ079C	Middle Waste	dolostone	5	1.6
wpsJ070C	Middle Waste	mudstone	11	2.8
wpsJ067C	Middle Waste	siltstone	17	2.2
wpsJ065C	Middle Waste	mudstone	20	2.6
wpsJ063C	Middle Waste	mudstone	11	2.6
wpsJ061C	Middle Waste	mudstone	14	2.2
wpsJ059C	Middle Waste	mudstone	10	2.0
wpsJ057C	Middle Waste	mudstone	28	2.5
wpsJ054C	Middle Waste	mudstone	3	0.0
wpsJ052C	Middle Waste	mudstone	15	2.7
wpsJ050C	Middle Waste	mudstone	26	2.2
wpsJ048C	Lower Ore	siltstone	46	2.3
wpsJ047C	Lower Ore	phosphorite	58	2.4
wpsJ045C	Lower Ore	phosphorite	60	2.4
wpsJ040C	Lower Ore	phosphorite	78	2.2
wpsJ037C	Lower Ore	phosphorite	34	2.4
wpsJ035C	Lower Ore	phosphorite	54	2.2
wpsJ034C	False Cap	siltstone	18	1.1
wpsJ031C	Lower Ore	phosphorite	63	1.3
wpsJ025C	Lower Waste	siltstone	1	0.0
wpsJ023C	Lower Ore	phosphorite	69	1.9
wpsJ022C	Lower Waste	siltstone	5	0.0
wpsJ021C	Lower Waste	mudstone	38	1.0
wpsJ020C	Lower Waste	mudstone	49	1.7
wpsJ018C	Lower Ore	phosphorite	60	2.0
wpsJ017C	Lower Ore	dolostone	15	2.4
wpsJ014C	Lower Ore	phosphorite	65	2.8
wpsJ011C	Cap Rock	mudstone	29	2.0
wpsJ008C	Lower Ore	phosphorite	86	2.4
wpsJ006C	Footwall	siltstone	25	2.3
wpsJ003C	Footwall	dolostone	0	0.0
wpsJ002C	Footwall	dolostone	1	0.0
wpsJ0.5C	Fish-scale bed	phosphorite	83	0.8
wpsJ-01C	Grandeur	dolostone	1	0.0
wpsJ-03C	Grandeur	dolostone	0	0.0
wpsJ-05C	Grandeur	dolostone	1	0.0

Table 2b: Data for CO_3^{2-} substitution in fluorapatite for section J individual samples based on the equation by Schuffert and others (1990):

$$y = 10.643x^2 - 52.512x + 56.986$$

Where y = the wt. % CO_3^{2-}, and x = $\Delta 2\theta_{(004)-(410)}$ for fluorapatite, as calculated by cell parameters obtained from Rietveld analysis.

WUSP Sample	Unit	Lithology	% apatite	CO_3^{2-} (wt %)
wpsJ188.2K	Rex Chert	chert	39	2.0
wpsJ186.8K	Upper Waste	phosphorite	56	1.8
wpsJ186.2K	Upper Waste	phosphorite	71	2.7
wpsJ185.9K	Upper Waste	phosphorite	71	2.5
wpsJ185.2K	Upper Waste	phosphorite	76	2.9
wpsJ175.7K	Upper Waste	mudstone	9	0.4
wpsJ174.7K	Upper Waste	mudstone	16	2.0
wpsJ170.3K	Upper Waste	mudstone	36	1.4
wpsJ162.4K	Upper Ore	phosphorite	89	2.4
wpsJ161.8K	Upper Ore	phosphorite	66	2.8
wpsJ152.2K	Upper Ore	phosphorite	78	2.9
wpsJ150.5K	Upper Ore	phosphorite	72	2.6
wpsJ146.2K	Middle Waste	mudstone	39	2.8
wpsJ141.1K	Middle Waste	dolostone	23	2.0
wpsJ140.1K	Middle Waste	mudstone	30	2.0
wpsJ139.8K	Middle Waste	mudstone	24	2.7
wpsJ138.6K	Middle Waste	mudstone	33	2.5
wpsJ138.4K	Middle Waste	mudstone	49	1.8
wpsJ138.2K	Middle Waste	mudstone	47	2.9
wpsJ137.3K	Middle Waste	mudstone	72	2.4
wpsJ137.1K	Middle Waste	mudstone	14	0.0
wpsJ136.8K	Middle Waste	dolostone	20	3.4
wpsJ136.4K	Middle Waste	mudstone	49	2.4
wpsJ135.7K	Middle Waste	mudstone	67	2.5
wpsJ135.4K	Middle Waste	mudstone	60	2.6
wpsJ135.2K	Middle Waste	mudstone	29	2.2
wpsJ135.0K	Middle Waste	mudstone	18	1.6
wpsJ127.7K	Middle Waste	siltstone	0	0.0
wpsJ117.6K	Middle Waste	mudstone	59	2.5
wpsJ109.9K	Middle Waste	phosphorite	3	0.0
wpsJ107.9K	Middle Waste	phosphorite	62	2.1
wpsJ105.8K	Middle Waste	mudstone	27	2.2
wpsJ105.4K	Middle Waste	mudstone	16	2.0
wpsJ104.9K	Middle Waste	mudstone	0	0.0
wpsJ103.3K	Middle Waste	mudstone	44	2.6
wpsJ97.2K	Middle Waste	dolostone	3	0.0
wpsJ96.5K	Middle Waste	carbon seam	27	2.6
wpsJ96.4K	Middle Waste	dolostone	0	0.0
wpsJ95.4K	Middle Waste	carbon seam	35	2.7
wpsJ95.3K	Middle Waste	dolostone	1	0.0

Table 2b: (continued)

WUSP Sample	Unit	Lithology	% apatite	CO_3^{2-} (wt %)
wpsJ94.9K	Middle Waste	mudstone	30	1.7
wpsJ94.0K	Middle Waste	mudstone	34	2.2
wpsJ93.8K	Middle Waste	mudstone	34	2.7
wpsJ93.4K	Middle Waste	mudstone	13	2.6
wpsJ93.13K	Middle Waste	dolostone	0	0.0
wpsJ85.1K	Middle Waste	dolostone	1	0.0
wpsJ84.7K	Middle Waste	dolostone	1	0.0
wpsJ83.8K	Middle Waste	carbon seam	35	1.9
wpsJ83.57K	Middle Waste	mudstone	50	2.1
wpsJ82.53K	Middle Waste	mudstone	31	1.9
wpsJ82.33K	Middle Waste	mudstone	10	0.0
wpsJ82.27K	Middle Waste	mudstone	16	1.8
wpsJ82.2K	Middle Waste	mudstone	33	1.9
wpsJ82.1K	Middle Waste	mudstone	34	2.7
wpsJ82.07K	Middle Waste	dolostone	20	2.9
wpsJ81.7K	Middle Waste	dolostone	19	2.0
wpsJ81.1K	Middle Waste	dolostone	1	0.0
wpsJ75.2K	Middle Waste	mudstone	8	0.0
wpsJ73.3K	Middle Waste	mudstone	18	1.4
wpsJ68.1K	Middle Waste	mudstone	43	2.4
wpsJ62.7K	Middle Waste	mudstone	12	2.0
wpsJ56.0K	Middle Waste	mudstone	13	2.2
wpsJ50.8K	Middle Waste	mudstone	6	0.0
wpsJ36.6K	Lower Ore	phosphorite	73	1.8
wpsJ36.2K	Lower Ore	phosphorite	80	2.5
wpsJ35.7K	Lower Ore	phosphorite	65	1.9
wpsJ27.0K	Lower Ore	phosphorite	88	1.4
wpsJ18.8K	Lower Ore	phosphorite	55	1.6
wpsJ8.8K	Lower Ore	phosphorite	82	2.3
wpsJ8.7K	Lower Ore	phosphorite	83	3.1
wpsJ8.6K	Lower Ore	phosphorite	75	2.3
wpsJ8.3K	Lower Ore	siltstone	89	2.6
wpsJ8.2K	Lower Ore	siltstone	75	2.5
wpsJ8.0K	Lower Ore	siltstone	80	2.1
wpsJ7.6K	Lower Ore	siltstone	80	2.5
wpsJ7.3K	Lower Ore	siltstone	0	0.0
wpsJ5.4K	Lower Ore	siltstone	1	0.0
wpsJ2.85K	Lower Ore	dolostone	0	0.0
wpsJ1.89K	Lower Ore	dolostone	0	0.0
wpsJ1.6K	Lower Ore	dolostone	1	0.0
wpsJ1.26K	Lower Ore	dolostone	0	0.0
wpsJ0.8K	Lower Ore	dolostone	0	0.0
wpsJ0.2K	Lower Ore	phosphorite	76	2.4
wpsJ-3.2K	Grandeur	dolostone	2	0.0
wpsJ-6.5K	Grandeur	dolostone	0	0.0

Figure 4: Carbonate substitution for phosphate in fluorapatite reported in weight percent for samples from the central part of Rasmussen Ridge including the measured stratigraphic sections J (including channel and individual samples), B, and A. Carbonate content is determined using the equation of Schuffert and others (1990): $y = 10.643x^2 - 52.512x + 56.986$

Where y = the wt. % CO_3^{2-}, and x = $\Delta 2\theta_{(004)-(410)}$ for fluorapatite, calculated by cell parameters obtained from Rietveld analysis. Section A and B data are from modified from Knudsen and others (2000). While the sections cannot be directly correlated stratigraphically, recognized ore and waste zones, constant between sections, are noted for reference.